# Development of early calcareous nannoplankton in the Northern Calcareous Alps (Austria) in the Upper Triassic

Isaline Demangel, Agnes Zsofia Kovacs, Sylvain Richoz, Silvia Gardin, Leopold Krystyn, Andre Baldermann, Werner Piller

https://doi.org/10.1016/j.gloplacha.2020.103254

# Development of early calcareous nannoplankton in the Northern Calcareous Alps (Austria) in the Upper Triassic

Isaline Demangel[1, 2], Zsofia Kovacs[1, 2], Sylvain Richoz[1, 2], Silvia Gardin[3], Leopold Krystyn[4], Andre Baldermann[5], Werner E. Piller[1]

*1 Institute of Earth Sciences, University of Graz, NAWI Graz Geocenter, Graz, Austria*
*2 Department of Geology, University of Lund, Lund, Sweden*
*3 Centre de Recherche sur la Paléobiodiversité et les Paléoenvironnements, Sorbonne Université, Paris, France*
*4 Department of Paleontology, University of Vienna, Vienna, Austria*
*5 Institute of Applied Geosciences, University of Technology, NAWI Graz Geocenter, Graz, Austria*

Coccolithophorids are considered to be the most productive calcifying organisms on Earth and therefore to play an important role in the marine carbon cycle, as a biological pump and regulator of oceanic alkalinity. One particular point of interest is the emergence of the calcifying plankton in the marine ecosystem shifting the major carbonate production from the shallow seas to the open marine realm. This major event occurred during the Triassic period. This study focus on Steinbergkogel sections (Austria), a candidate for the Global Stratotype Section and Point (GSSP) for the Norian–Rhaetian boundary, corresponding to a hemipelagic paleoenvironment on a topographic high and a paleolatitude around 30°N. Using a Scanning Electron Microscope for detail investigation we better define the timing and evolution of the pelagic calcifiers' emergence. The lowest occurrence of *coccoliths sp.* leads in the middle Norian (Alaunian). The oldest *C. minutus* and *A. koessenensis* were observed in the Upper Norian (Sevatian). And the lowest occurrence of *C. primulus* could be defined from the Lower Rhaetian. Those observations show a slow evolution, during millions of years, of the first coccolithophorids from the ancestor *C. minutus* to *A. koessenensis* and then *C. primulus*. Using Inductively Coupled Plasma Optical Emission Spectrometry (ICP-OES) analyses we show a little diagenetic overprint impacting only the preservation of the calcareous nannofossils via partial dissolution and recrystallization. This allow us to be confident in the quantitative estimation of the volume and paleo-fluxes of the calcareous nannofossils during this bio-event that show the dominance of *P. triassica* in the Northern Calcareous Alps and their increase in abundance slightly above the Norian/Rhaetian boundary.

Keywords: Coccolithophorids; Calcareous nannofossils; *Prinsiosphaera triassica*; Quantification; Evolution.

## *1.* Introduction

Calcareous nannoplankton were described for the first time in 1836 by the German biologist Ehrenberg, as small "flat", elliptical discs of "agaric-mineral" (Tyrrell and Young, 2009). After this

first discovery, several researches in the Western Tethys (South Germany, Calcareous Alps of Italy and Austria) report the description and the first occurrence datum of the calcareous nannofossils during the Upper Triassic. Concerning the coccolithophorids, Prins (1969) described the first *Crucirhabdus primulus* from lower and middle Liassic sediments in England, France and Western Germany. Later Jafar (1983) described the first *Crucirhabdus minutus* and record specimens of *C. primulus* in section of southern Bavaria (Germany) from the base of the Rhaetian. Two years later, Bown (1985) reports the first *Archaeozygodiscus koessenensis* from the *marshi* Zone (Late Rhaetian) in an Austrian section. Gardin et al., (2012) reviewed all the different Upper Triassic reports of coccolithophorids to conclude for all of them to a Rhaetian age. In the same study, they reported the oldest occurrences of *C. minutus* and of *Coccoliths spp.* until now. Investigation at Steinbergkogel (Austria), a GSSP candidate for the Norian/Rhaetian boundary, permitted to find *C. minutus* specimens just above the Norian/Rhaetian boundary and tiny *coccoliths spp.* in the uppermost Norian.

From the Upper Triassic onward, dinocysts, nannoliths and coccoliths composed a large part of the phytoplankton's total productivity, accumulating until today a huge amount of calcium carbonate on the ocean floor. This initiation of the pelagic carbonate production is a major change in the ocean chemistry representing the shift from the "Neritan Ocean" with infinite saturation dominated by biogenic shallow-water $CaCO_3$ to the "Cretan Ocean" with low saturation dominated by pelagic $CaCO_3$ and very stable deep ocean [$CO_3^{2-}$] (Zeebe and Westbroek, 2003). To understand how the calcifying organisms will evolve with the current ocean acidification, the geological records can complement modern data by providing long time scale records. This critical nannoplankton appearance and evolution was quantified in two tethysian basins in South Italy (Preto et al., 2013a) with the main Rhaetian nannoliths, *Prinsiosphaera triassica,* building 0 to 10% of the rock volume during the Norian, 20 to 40 % in the middle Rhaetian and up to 60% in the upper Rhaetian, while coccolithophores remained subordinate. At Steinbergkogel (Austria), Gardin et al. (2012) published a semi-quantitative estimation of the calcareous nannofossils abundance in the Upper Triassic showing only few nannoliths and calcareous cysts in the mid – to late Norian and a significant increase in *Prinsiosphaera triassica* around the Norian-Rhaetian boundary.

Gardin et al. (2012) and Preto et al. (2013a) improved the understanding of the early evolution of the calcareous nannofossils. To verify if the observations from the Italian sections are regional or global and to investigate the importance of the bathymetrical differences point out by Preto et al. (2013a) further investigation are however needed. Among other Steinbergkogel needed a detail quantification rather than semi-quantitatively estimation and a control on diagenesis. In this context, our study at Steinbergkogel first focuses on the eventual impact of diagenesis on the preservation and abundance of the calcareous nannofossils. The second aims is to proceed to detail investigations on the First

Occurrence Datum (FOD) of the coccolithophorids by looking at middle to lower Norian sediment. The final aim is to perform a quantitative estimation of the volume and palaeo-fluxes of the calcareous nannofossils during the Upper Triassic in Austrian hemipelagic highs.

## *2.* Geological settings

During the Upper Triassic (237-201.3 Ma; International Chronostratigraphic Chart v2017/02), the Northern Calcareous Alps (NCA) were located on the Western Tethys margin around 30°N (Fig 1) and registered tropical climate with the maximum activity of the mega-monsoons system (Robinson, 1973; Preto et al., 2010) modulated by Milankovitch cycles (Ogg, 2012). The Austrian Northern Calcareous Alps were during Middle and Upper Triassic a region of very large carbonate platforms (Richoz and Krystyn, 2015). During the late Carnian, the widespread Dachstein platform developed above the siliciclastic deposit link to the Carnian Humid Event (e.g. Ruffels et al., 2015). This platform is composed of intra-platform basins, large lagoons extending toward the south-east and fringing reefs open to the ocean, where Hallstatt facies pelagic limestones developed (Richoz and Krystyn, 2015). This deep shelf environment shows lateral and successive differences between massive light limestone and red condensed limestone (Krystyn, 1980). Indeed, the region was subject to diapirism of Permian evaporites creating hemipelagic high environments, where the red Hallstatt limestones were deposited at the top (Fig 1). This formation ends due to increasing terrigenous input during the early Rhaetian corresponding to the marly Zlambach Formation. The most recent study on the basin, conducted by Kenter and Schlager (2009), proposed a depth of at least 300 meters, but probably 500m, based the clinoform geometry, sediment composition and geopetal fabrics in the Dachstein platform margin.

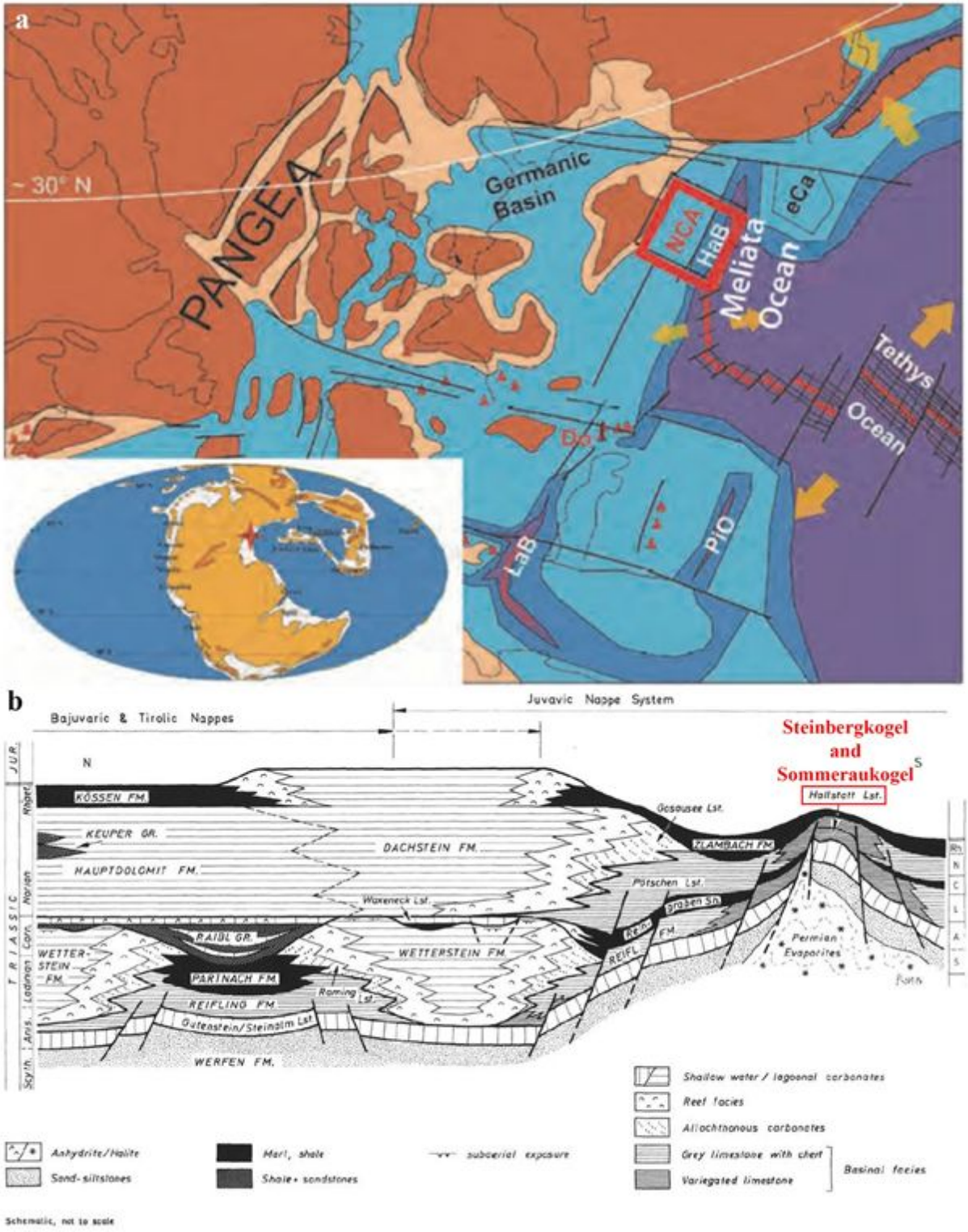


Fig 1 – a) Palaeogeographic reconstruction of the global world and the Western Tethyan margin during the Upper Triassic (from Hornung et al., 2007). With NCA = Northern Calcareous Alps, eCA = East Carpathians, HaB = Hallstatt Basin, Do = Dolomite, PiO = Pinde Ocean, LaB = Lagonegro Basin. b) Triassic stratigraphy of the NCA (middle sector) (from Mandl, 2000).

Nowadays, the NCA are formed by three nappes complexes (Bajuvaric, Tirolic, and Juvavic), which extended on 500 km long and 20-50 km wide along Austria (Fig 2). In the middle of this belt,

near Hallstatt lake, around 1245m above sea level the Hallstatt Limestone and marly Zlambach Formation are visible at Sommeraukogel section and in an old quarry at Steinbergkogel sections (Fig 2). Described in details by Krystyn (1980), Sommeraukogel corresponds to the section with the oldest sediments, from the Anisian to the Norian. Our study focuses there only on the Alaunian 2 (sub-zone IV, Middle Norian) consisting of red Hallstatt limestone, characterized by the presence of *Halorites* ammonoids and of the conodonts *E. abneptis* and *E. vrielyncki*. A fault cut the top of the section and the Alaunian 3 is missing in this area. Few meters above, after the fault, start at the coordinates 47°33'50''N / 13°37'34''E the proposed Norian/Rhaetian boundary GSSP candidate, Steinbergkogel section (Fig 2). From the Upper Norian (Sevatian) to the Lower Rhaetian, the profile is composed of four successive and overlapping sub-sections. First, ST4 extend from the *E. bidentata* conodont zone to the *E. bidentata – M. hernsteini* Zone and is composed of 23 m mostly massive red Hallstatt limestone beds. This facies is still visible above within the first beds of the overlapping section, STK 1A. From the bed 107, the limestone changed in color to grey and contains high bioclastic fossils content until the bed 112. The bed 111A which records the FAD of *Misikella posthernsteini* is the proposed Norian/Rhaetian boundary. This sub-section of 3 m high in total ends with grey/reddish limestone. It is overlapped by the section STK 1B/C which presents nodular limestone and marls indicating a low sedimentation rate and compaction after deposition (Hüsing et al., 2011). The section ends with the transition to the grey marls of the Zlambach Formation linked with an increased sedimentation rate due to a higher level of siliciclastic input (Krystyn et al., 2007a).

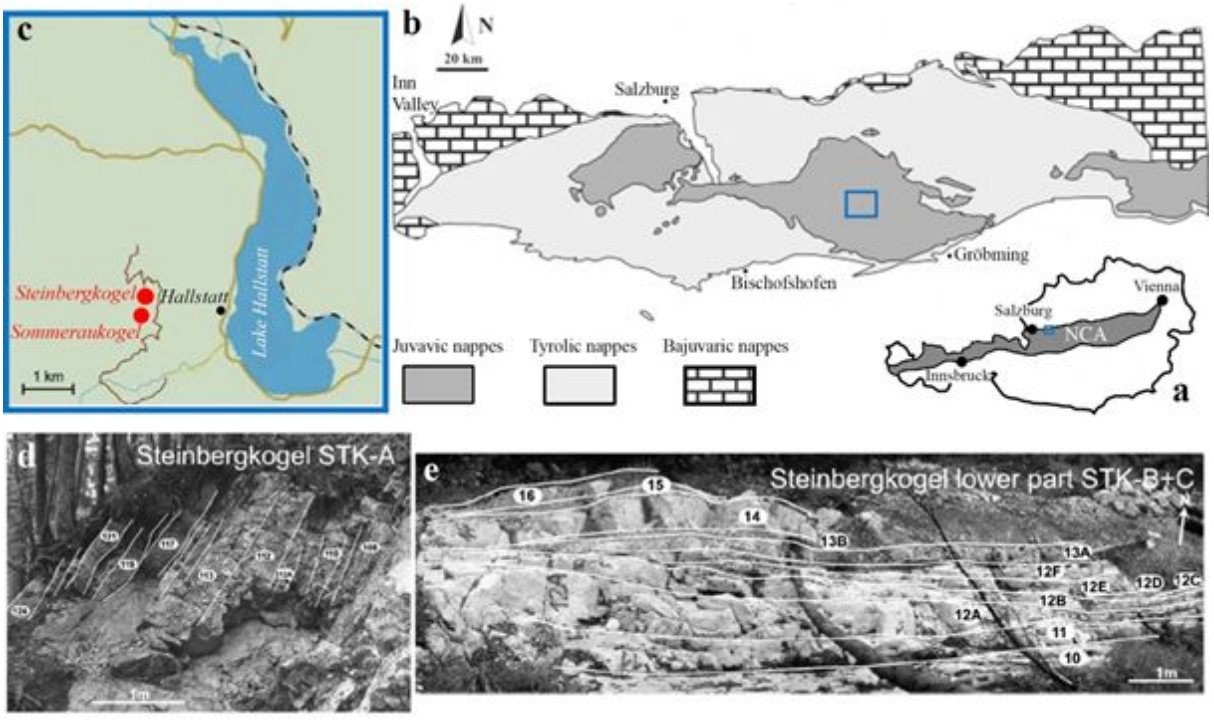

Fig 2 – a) Distribution of the NCA in the frame of Austria (modified after Schorn et Neubauer, 2014). b) Overview of the Austroalpine units in the central NCA (Leitner et al., 2011). c) Location of the studied sections near Hallstatt in Austria (modified after Gardin et al., 2012). d) Photograph of the STK 1A subsection of Steinbergkogel (from Hüsing et al., 2011). e) Photograph of the lower part of the STK 1B/C subsections of Steinbergkogel (from Hüsing et al., 2011). Numbers in the photographs correspond to the numbers indicated in figure 4 from Krystyn et al. (2007a).

Hallstatt limestones record an abundant and very diverse invertebrate fauna such as the 500 species of cephalopods mostly orthoceratids, nautiloids and ammonoids described in details by Mojsisovics (1873-1902). The bivalves, in particular halobiids, have been described by Kittl (1912). Gastropods and brachiopods were respectively described by Koken (1897) and Bittner (1890). Finally, few occurrences of reefal organisms are registered (Krystyn, 1980; Krystyn et al., 2007b; Richoz and Krystyn, 2015). The Hallstatt Formation is also composed of diverse microfauna including benthics foraminiferas, sponges spicules dominating the Rhaetian grey limestones (Richoz and Krystyn, 2015), radiolarians, echinoderms (crinoids and echinoids), holothurian sclerites and conodonts (Krystyn, 1980, Mosher 1968 and Krystyn et al., 2007a, b). The conodonts and ammonoids have been used in parallel of abiotic stratigraphic tools (stable isotopes, magnetostratigraphy) for time control and high-resolution correlation (Fig 3) (Krystyn et al., 2007b, Hüsing et al., 2011). Normal marine salinity occurs throughout all sections as indicated by the continuous presence of stenohaline sessile organisms (echinoderms). The diversity of benthic species link with the high density of traces fossil indicates oxic conditions at the sea bottom (Richoz and Krystyn, 2015).

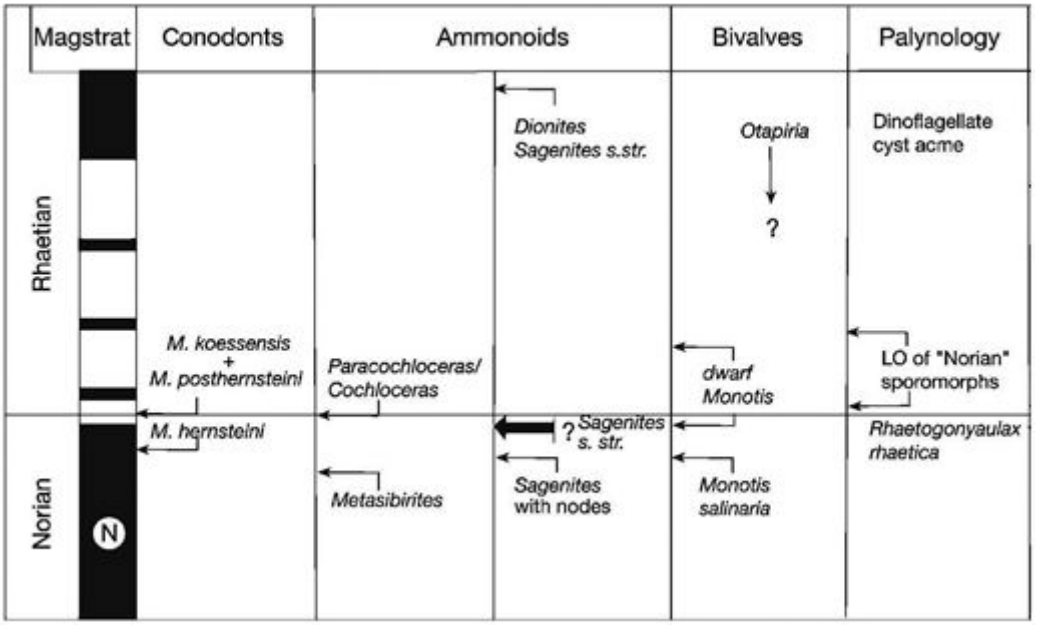

Fig 3 – Correlation of bioevents around the Norian/Rhaetian boundary at Steinbergkogel.

### 2.1 Description of the Upper Triassic calcareous nannofossils:

The GSSP candidate at Steinbergkogel is described as an excellent section for the Norian/Rhaetian boundary by Krystyn et al. (2007 a,b) but also as the greatest place for calcareous nannofossils birth investigation by Gardin et al. (2012). Most common calcareous nannofossils of the Upper Triassic (Fig 4) include the two nannoliths, *Prinsiosphaera triassica* and (*Eo*-)*conusphaera zlambachensis*, the three coccoliths, *Archaeozygodiscus koessenensis*, *Crucirhabdus primulus*, *Crucirhabdus minutus*, and the three calcareous cysts *Obliquipithonella spp.*, *Orthopithonella spp.* and *Thoracosphaera spp*.

*Prinsiosphaera triassica* was originally described by Jafar (1983) as a spherical to hemispherical solid, containing a depression at one end and composed of thin, tabular calcite rhombohedral arranged in parallel groups randomly positioned to form the nannoliths. Nevertheless, *P. triassica* has a large diversity of forms. Due to this, Jafar (1983) described five subspecies, *Prinsiosphaera triassica hyalina*, *Prinsiosphaera triassica punctata*, *Prinsiosphaera triassica perforata*, *Prinsiosphaera triassica crenulata*, *Prinsiosphaera triassica noeliae*. For Janofske (1987), those sub-species are diagenetic shapes of *P. triassica*, *Orthopithonella geometrica* or *Obliquipithonella rhombica*. Bralower (1991), explained this diversity as an etching effect defining four stage of preservation going from the entire smooth outer layer visible to the etched inner layer visible characterized by the tabular calcite groups randomly positioned. *P. triassica* presents also a broad variation of size, first, Bralower (1991) report a diameter ranging from 6 µm during the middle Norian to 9 µm during the Upper Rhaetian. In 2010, Clémence et al., described a size reduction during the latest Rhaetian and outlining three size groups, large (10-8 µm), medium (7-6 µm) and small (<5 µm) regarding the assemblages presents. *P. triassica* is the main carbonate producer species among the nannofossils during the Upper Triassic in the western Tethys (Preto et al., 2013b).

The second nannoliths, (*Eo*-)*conusphaera zlambachensis* (family Euconusphaeraceae) was first described by Moshkovitz (1982) as an elongated cone, truncated at both ends, composed in the inner part of 35-40 radial, inclined calcitic lamellae sinistrally turning and in the outer part of long smooth plates. Later, Bralower (1991) suggest an evolution from a stubby shape with an average length of 3µm to an elongated form with an average length of 5µm.

Regarding the calcareous cysts, the three species have been all originally described by Jafar (1983). *Thoracosphaera spp.* corresponds to a bowl-or hat-shape with a size between 5 to 13 µm. Living specimens are known to be a dinophyte which secretes a calcareous cell wall in the vegetative life phase. *Orthopithonella spp.* is a spherical solid with element perpendicular to the wall and a

diameter around 9 µm. *Obliquipithonella spp.* is nearly similar to the previous species but possesses element oblique to the wall and the size is smaller with diameter around 6 µm.

Concerning the Upper Triassic coccoliths, *Crucirhabdus primulus* have been the first described (Prins 1969). This species with a size between 3 to 5 µm present an elliptical shape. Rood et al., (1973) and Janofske (1987) describe a loxolith rim with imbricated elements. Bown (1987), and Bralower (1991) define the species with vertical to subvertical elements, corresponding to a protolith rim. The central area of the rim is bearing a cross. Later, *Crucirhabdus minutus* have been described by Jafar (1983) as a tiny elliptical coccolith with a size range between 1.6 to 2.4 µm. The inner rim present a cross supporting a central spine. Concerning the rim elements orientation, Bown (1985) defined a protolith rim, while Bralower (1991) outlined both protolith and loxolith possibility. Finally, *Archaeozygodiscus koessenensis,* have been later described by Bown (1985) as an elliptical coccolith with loxolith structure rim imbricating in an anticlockwise direction and a size ranging from 1.9 to 3.2 µm. The inner part holds a thick bar with a circular hole in the middle. About their evolution, Bralower supported that *C. primulus* is the ancestor of a lineage which gave rise to *C. minutus* and *A. koessenensis*. He justified this lineage with the row of apparition in the sediments and by the development of the rim structure, which is for him, protolithic in *C. primulus*, protolithic or loxolithic in *C. minutus* and loxolithic in *A. koessenensis*. In older studies, Thierstein (1976), Jafar (1983), Bown (1987) and recently Gardin et al., (2012) proposed an other lineage with *C. minutus* giving the rise to *C. primulus*, given an apparition order in contrary to Bralower (1991). About their First Occurrence Datum, the most recent and biostratigraphically controlled report until now is given by Gardin et al., 2012 (see also Richoz and Krystyn, 2015) from an investigation at Steinbergkogel section. They observed indeterminate coccoliths spp. from bed 106 of STK 1A (STK 1A/106) just below the Norian/Rhaetian boundary. The FO of *C. minutus* is defined just above this boundary at STK 1A/112A and STK 1C/12E. The FO of *C. primulus* appeared later in the lower Rhaetian at STK 1B/28.

## *1.* Materials and methods

### a. SEM sample preparation and quantification:

Through all the sections (Sommeraukogel, Steinbergkogel sections) (Figure 4) described above, a total of 26 samples have been carefully investigated under the SEM. In details, 3 samples of Sommeraukogel, 12 samples of ST4, 5 samples of STK 1A and 6 samples of STK 1B/C were observed. To select the studied samples an interval of 2 m for Sommeraukogel and ST 4, and of 1m for STK 1A, 1B/C have been chosen. In parallel, to check if lateral variations exist, beds 113 B and 12E respectively from section STK 1A and STK 1B/C, have been analysed regarding the abundance

of nannofossils in differents lateral samples. For the bed 113 B (STK 1A), 6 samples have been investigated corresponding to the following lateral positions: 0m, 0.6m, 1m, 1.5m, 1.9m, 2.5m. For the bed 12E (STK 1B/C), 7 samples have been studied respectively at 1m, 2m, 3m, 4m, 5m, 6m, and 8m.

The use of SEM and of solid rocks was chosen instead of the more widely use smear/settling slide, because after several observations of smear slides under both light microscope and SEM no calcareous nannofossils were found. Most probably due to the extremely compact limestone enclosing the nannofossils and prevents their single "extraction" during the sample preparation. Thus, the sample preparation methods described by Preto et al. (2013a, b) have been followed with slight modifications regarding our facies and locality. Indeed, after a qualitative investigation of some solid samples with the Hitachi Tabletop Microscope TM3000 (Sorbonne University, UMP CNRS 7207 CR2P, Paris, France), the samples were cut in blocks of $1cm^2$. Then, they were polished with 600 and 1200 diamonds discs using deionized water. After, the blocks were etched for 15 seconds in 0.1% HCl, and cleaned for 7 seconds in ultrasonic bath with distillate water. The samples were dried for the night in the air oven at 50°C and finally coated with 1nm of platinum/palladium using Cressington Sputter Coater 208HR.

The quantitative estimation was done with a TESCAN MIRA 3 at Lund University. To reduce the effects of samples heterogeneity, surfaces perpendicular to the bedding were cut (Chayes, 1964). Also, for two samples two transects, 1cm straight line along the block surface, were done to confirm the homogeneity of the quantification results. Each transects were observed to count each clear specimens, not including the potential small break part of *P. triassica*. The area of the frame (21.9 x 21.9 µm) was selected to be larger than the biggest calcareous nannofossils, in our case 11µm *P. triassica* specimens. The absolute number of nannofossils per cm² was calculated using the following equation of Bordiga et al. (2015) slightly modified:

$$x = (N \times A) \div (f \times n) \qquad \text{(equation 1)}$$

With x = absolute number of calcareous nannofossils per cm² of sediment; N = total number of individuals counted; A = area of the block (1 cm²); f = area of one frame in cm²; and n = number of frame analysed.

The total *P. triassica* carbonate flux could not be calculated in the standard way as described in several coccoliths carbonate fluxes studies (e.g., Young and Ziveri, 2000; Bornemann, 2003; Suchéras-Marx et al., 2014) due to the specific sample preparation method used in this study. Indeed, normally a certain amount of rock powder is used while we used solid piece of rock, thus the

nannoliths carbonate flux was calculated by multiplying the total number of *P. triassica* per $cm^3$ (**X**) by the sedimentation rate of 3m/My as estimated by Schlager (1961) for the Hallstatt Limestones. To obtain, X, the total number of the *P. triassica* in 1 $cm^3$, the following equation was use: $X = \frac{V\,rock \times 1}{x}$ (equation 2); with $V_{rock}$ ($cm^3$) = 1 $cm^3$ x mean diameter of *P. triassica* (cm) and x = absolute number of calcareous nannofossils per $cm^2$ of sediment, calculated previously. The diameter of specimens with distinct edges and clear half sphere visible were measured during the quantification and average for each samples.

In addition, to have an estimation of the percentage of *P. triassica* in the rock sample to compare to the study of Preto et al. (2013a), the total volume of *P. triassica* was calculated following the basic volume equation: $V_{total} = \frac{4}{3\pi r3} \times x$, (equation 3) with r = mean radius and x = absolute number of *P. triassica* per $cm^2$. Then the percentage was compute following: $\frac{V\,P.\,triassica \times 100}{V\,rock}$ (equation 4).

Stage
NORIAN
RHAETIAN
upper (Sevatian)
lower
middle (Alaunian)
Ammonoid zones
Paracochloceras suessi
Metasibirites spinescens
Halorites
Conodonts zones
M.posthernsteini - E.bidentata
Epigondolella bidentata
E.abneptis - E.vrielyncki
E.b - M.h
Formation
Zlambach Fm.
Hallstatt Formation
Lithology
Height (m)
25
20
15
10
5
0
several meters gap
3.5
2
0
Magneto-stratigraphy
Sections
STK 1B
STK 1A
STK 1C
ST 4
Sommeraukogel
Studied Samples
STK 1B/43
STK 1B/37B
STK 1B/29A
STK 1B/25B
STK 1B/19
STK 1B/10
STK 1A/120
STK 1A/113 A and B
STK 1C/12E
STK 1A/109 A
STK 1A/106 B
ST4/40
STK 1A/103
ST4/36
ST4/32
ST4/29
ST4/25
ST4/22
ST4/18
ST4/14
ST4/10
ST4/6
ST4/2
SO/17
SO/11
SO/1
Legend
Burrows
Nodular limestone
Bioclastic limestone
Lithoclastic limestone
Marls
Paracochloceras
Dionites
Metasibirites
Monotis salinaria
Halorites

Fig 4 – Schematic lithology, biomarkers zones, magnetostratigraphy from Krystyn et al., 2007b) and sample location of Sommeraukogel, ST 4, and STK 1A, 1B/C sections.

### b. Inductively coupled plasma atomic emission spectroscopy (ICP-OES):

In order to investigated the impact of the diagenesis on the preservation of the sediments, inductively coupled plasma atomic emission spectrometry analyses were conducted on 18 samples at the University of Technology in Graz (Austria), respectively two from Sommeraukogel section, five from ST4, seven from STK 1A and four from STK 1B. For the digestion 0.050g of powder sample were put in 50mL flask, then 5 drops of $HNO_3$ 69% and 50 mL of 2% $HNO_3$ bidestilled were added. After shaking, all the flasks were put in air oven at 80°C during 12h to digest the dolomite. Finally, the analyses were carried out using a Perkin Elmer OPTIMA 8300 DV at the Technical University of Graz, to obtain the total concentration of traces elements (Al, Ba, Ca, Cd, Co, Cr, Cu, Fe, K, Li, Mg, Mn, Na, Ni, Si, Sr, Zn) in each sample, after calibration of the data in ug/L or ppm. To estimate the amount of diagenesis the ratio traces elements were calculated as followed for e.g Mg/Ca:

$$\frac{\frac{Fraction\ of\ Mg\ (ppm)}{Atomic\ mass\ of\ Mg} \times 1000}{\frac{Fraction\ of\ Ca\ (ppm)}{Atomic\ mass\ of\ Ca}}$$

## *4.* Results

### a. Diagenesis:

The micrite of ten samples from the different sections were observed under the SEM to investigate dissolution or overgrowth patterns (Fig 5). From the oldest sections Sommeraukogel to mid ST4, all samples (SO/17, ST4/2, 4, 6 and 10) presents dissolution patterns, such as rough calcite spar crystal surface, micro-cracks and dissolution holes. In ST4, the overlying sample 12 possesses few dissolution features but mostly overgrowth patterns, like growth steps and smooth surface. Above, ST4/24 presents again only dissolution patterns. However, from the top of ST/4, samples ST4/38, STK 1A/119 and STK 1B/45 possess overgrowth pattern. Moreover, to evaluate the impact of the dissolution on the abundance of nannofossils, we observed specifically three samples, with high to low nannofossils abundance (ST4/2, 6 and 10). They present the exactly the same amount of dissolution patterns and the absence of overgrowth structures.

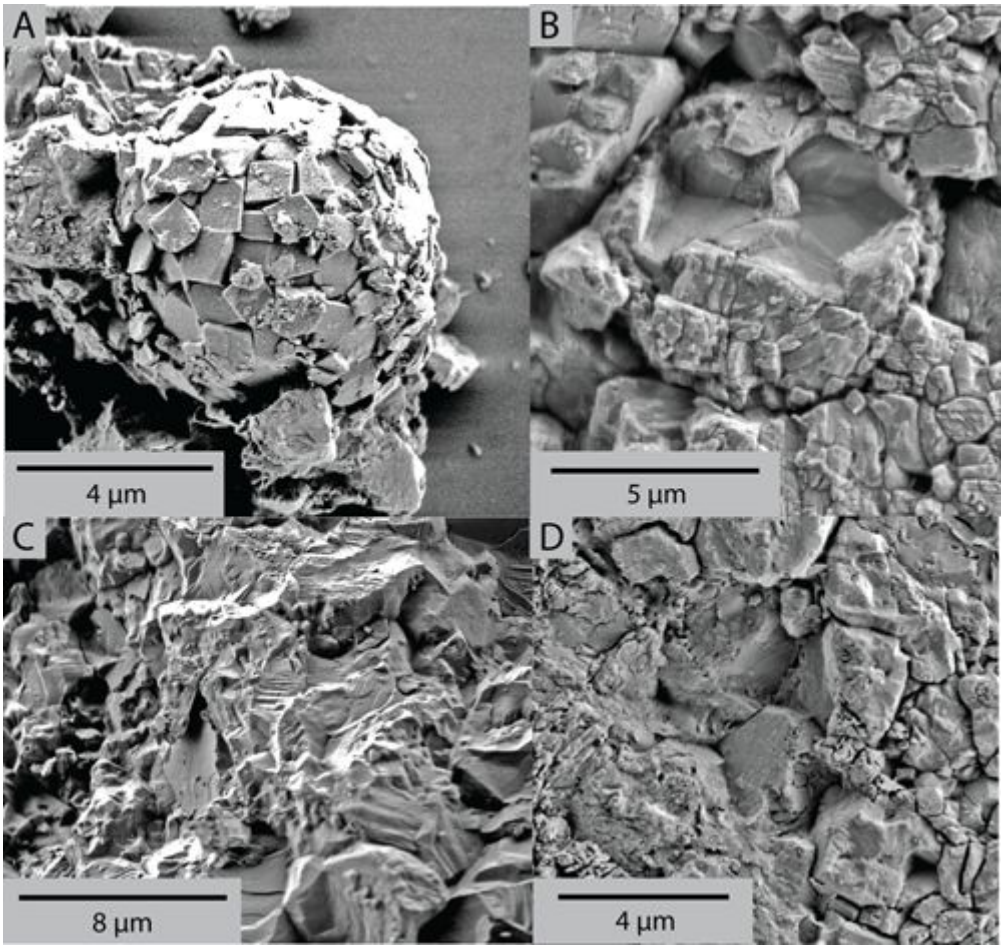


Fig 5 – SEM observation of the dissolution and overgrowth patterns. A- Recrystallized *P. triassica* from STK 1A/119A; B- *Orthopithonella* sp. refilled by secondary calcite crystal from STK 1B/29A; C- Overgrowth features in ST4/38; D- Dissolution patterns in ST4/2.

Elemental concentration results are presented as ratios of the element of interest with the calcium content of the same sample. The Al/Ca vs. Fe/Ca cross-plot shows strong correlation for all sections with $R^2 = 0.8424$ (Fig 6). This correlation between the aluminium and the iron values indicated that the Fe belongs to the silicates. Thus, in this case, the iron values cannot be integrated in the cross plot Na+Sr/Mn. This cross-plot reveals an increase of both values from the base of ST4 to the top. The middle Norian values at Sommeraukogel are exceptions, they do not follow this trend, the values are higher than at ST4. The Mn/Ca does not show any correlation with Al/Ca ($R^2 = 0.2148$). The Mn/Ca vs. Al/Ca cross-plot presents increasing values for both elements along all the sections, with however STK 1B presenting an anticorrelation (but based on only two points).

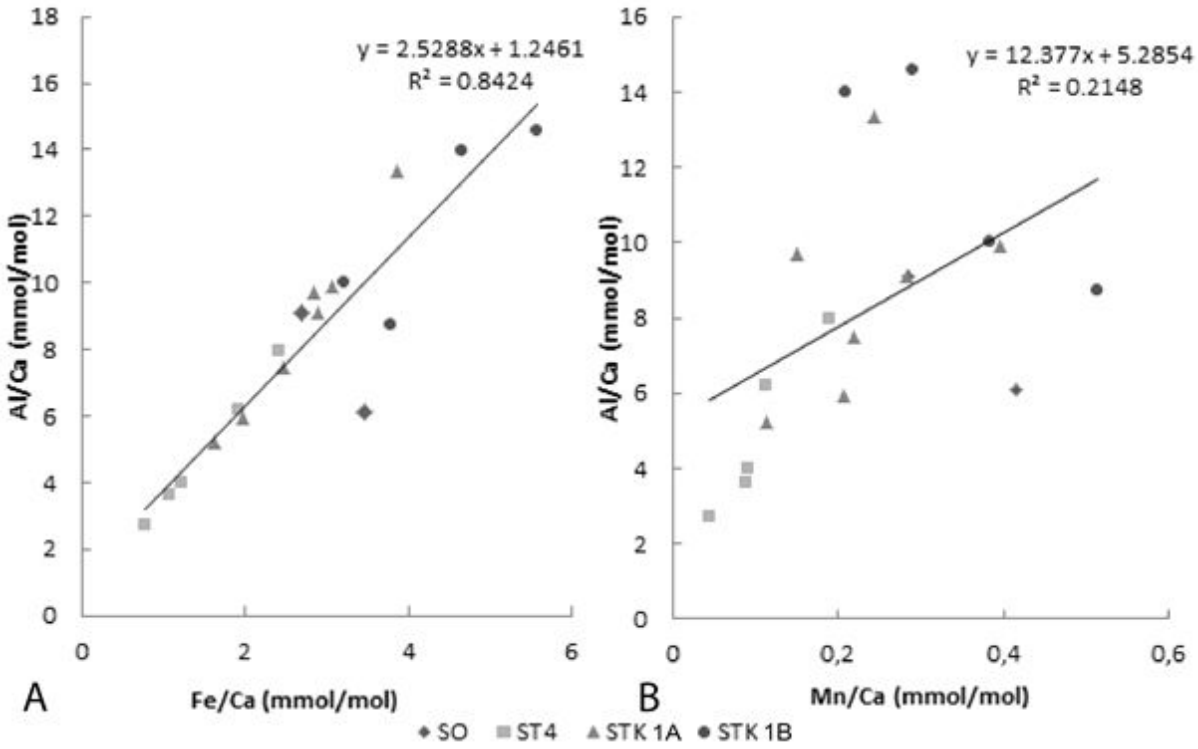


Fig 6 – Cross plot between A: Aluminium and Iron; B: Manganese for all the sections.

The cross plot between Na+Sr and Mn (Fig 7) presents values below 250 ppm for the manganese and below 500 ppm for Na+Sr for all the Steinbergkogel subsections. In details, at Sommeraukogel both values plot around 350 ppm for the Na+Sr and Mn concentrations are 130 and 210 ppm. Concerning ST4, the manganese values fluctuate between 22 and 91 ppm and the Na+Sr values vary broadly between 220 and 462 ppm. At STK 1A subsection Na+Sr concentration ranges between 315 and 495 ppm and Mn between 55 and 180. Finally, at STK 1B the values fluctuate between 250 and 350 ppm for Na+Sr and between 100 to 250 ppm for Mn. The strongest correlation was observed in ST4 subsection, in the other subsections negligible anticorrelation can be seen.

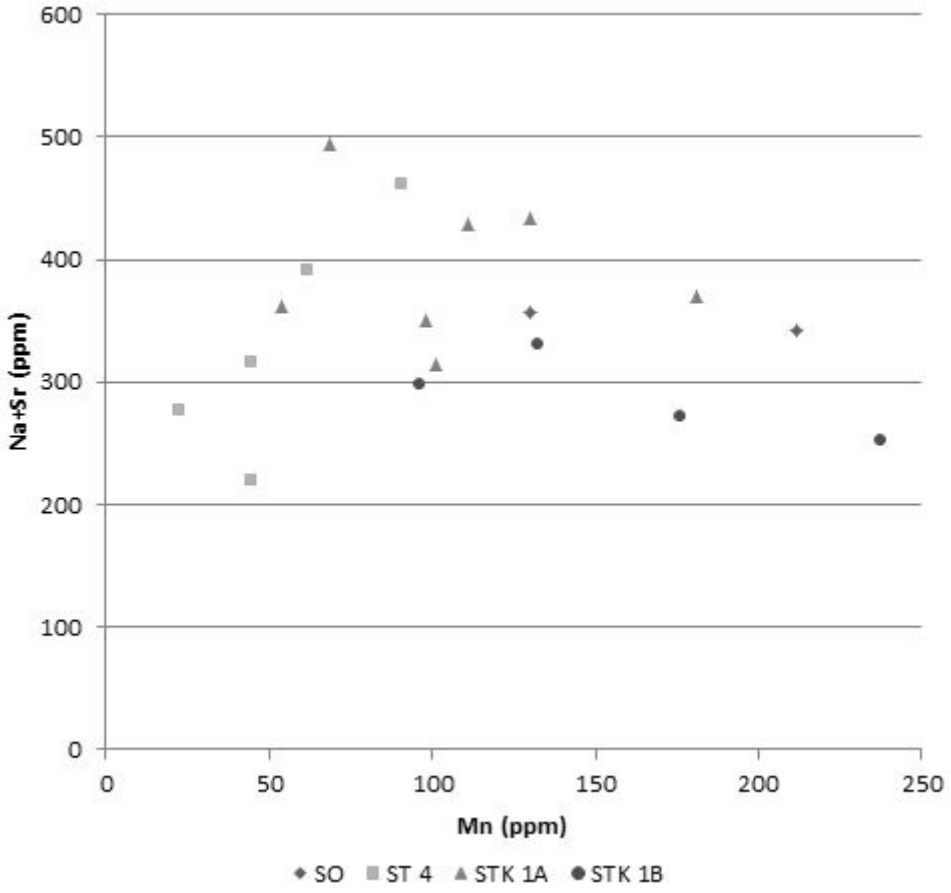


Fig 7 – Cross plot between Na+Sr and manganese for ST4 and STK 1A, 1B.

**b. Lowest Occurrence of the coccolithophorids and Upper Triassic nannofossils evolution:**

Calcareous nannofossils assemblages at Steinbergkogel are typical for Triassic sediment. The two nannoliths species *Prinsiosphaera triassica* and (*Eo*-) *Conusphaera zlambachensis* are present. The assemblage is also composed of two coccoliths species *A. koessenensis* and *C. minutus*, while *C. primulus* have not been observed in our study, but have been observed at Steinbergkogel by Gardin et al. (2012) and some specimens could not be identified at a species level. Then, calcareous cysts are present including *Thoracosphaera sp., Obliquipithonella sp.* and *Orthopithonella sp*. Finally, some undetermined calcispheres have been observed.

In general during the Upper Triassic *coccoliths spp*. evolved slowly, from sample SO/15 (middle Norian, Alaunian), they are rare with low abundance at the top of Sommeraukogel and base of ST4 section (Fig 12). During the rest of ST4, no specimen could be seen, then the abundance of *coccoliths spp.* increase from the beginning of section STK 1B corresponding to the lower Rhaetian. In detail, the specimen observed at SO/15 could not be identified but still represent the oldest

coccolith found until now (Fig 8, A). At the base of the next section, in ST4/2 (Sevatian, upper Norian), a well-preserved rim of *C. minutus* have been observed, corresponding to the oldest *C. minutus* ever identified (Fig 8, B). *A. koessenensis* has been identified in the sample ST4/6 still at the base of this Upper Norian section (Fig 8, C). From the middle Norian to the lower Rhaetian, the *coccoliths spp.* observed do not vary in size. *A. koessenensis* have stable size with a long axes lengths between 2.09 and 2.41 µm and short axes width between 1.36 and 1.77 µm. The *C. minutus* observed presents a length of 2.13 µm and width of 1.57 µm. The shape for each species is also similar along the sections, only the preservation states differ with on the one hand, good preservation of all the elements composing the rim and the central area (Fig 8, D), and on the other hand, with only the rim preserved in more or less good state (Fig 8, A).

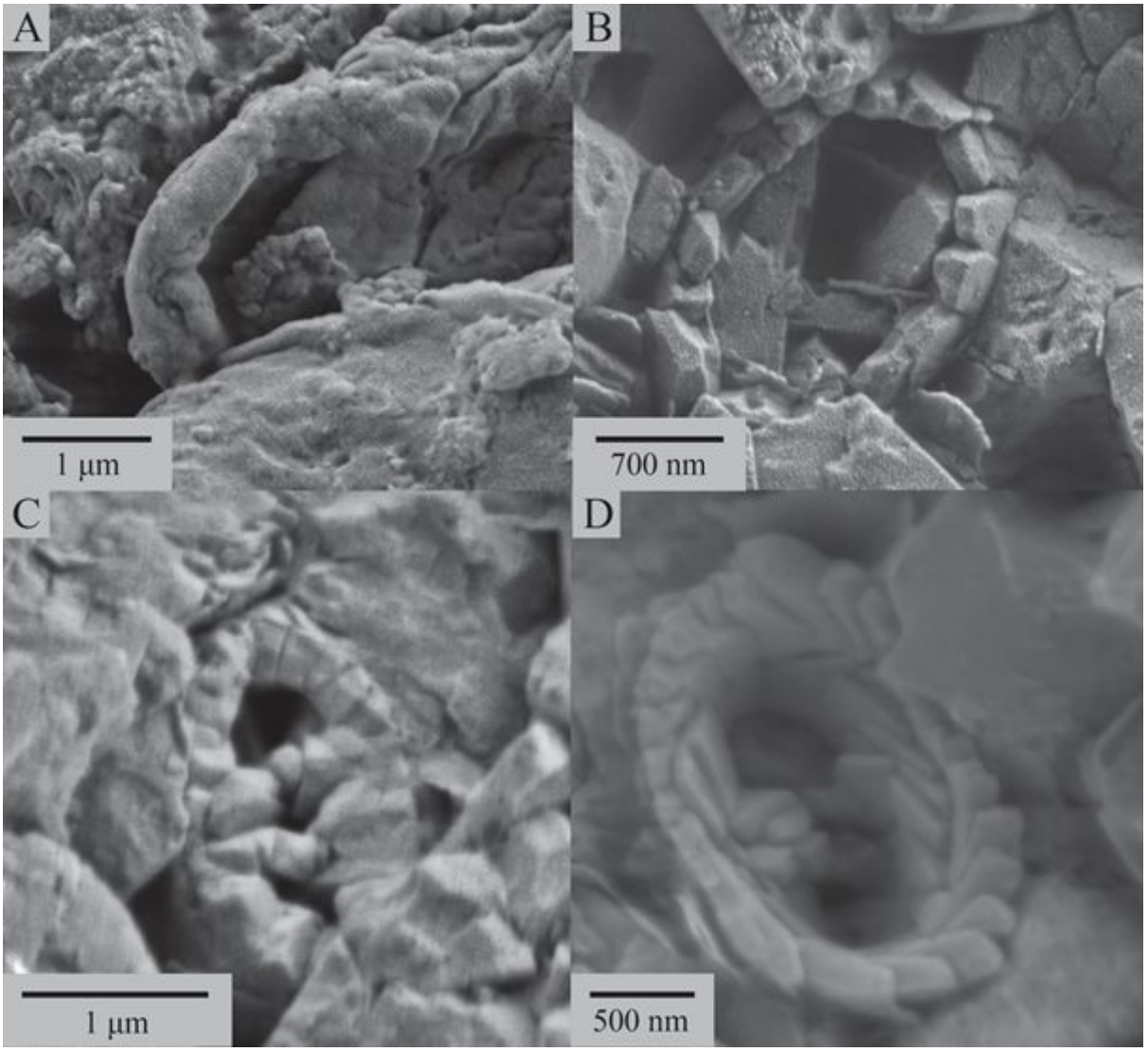


Fig 8 – SEM pictures representing A- Oldest coccoliths sp. from sample SO/15; B- Oldest *C. minutus* observed in ST4/2; C- Well-preserved *A. koessenensis* from ST4/6 ; D- *A. koessenensis* from STK 1B/37B.

Concerning the nannoliths, *P. triassica* specimens are present in every sample throughout all sections. They present a broad range of size going from 4.93 to 12.92 µm, but without any specific stratigraphic trend (Fig 9, A). Their shape is not changing, but with differences in preservation, three types have been observed. The most common one is when the *P. triassica* is broken in half and the inner part is visible with clear thin tabular calcite rhombohedral arranged in parallel forming group randomly positioned to the others (Fig 9, A). The second view, less observed is slightly similar to the previous one but instead of clear thin tabular calcite rhombohedral, there are blocks (Fig 9, B). The third one is when the specimen is not broken in half and thus the *P. triassica* is not flat as for the two previous views but is clearly rounded and thin tabular calcite arranged in parallel group are visible too, but with a clear arrangement between each group (Fig 9, C).

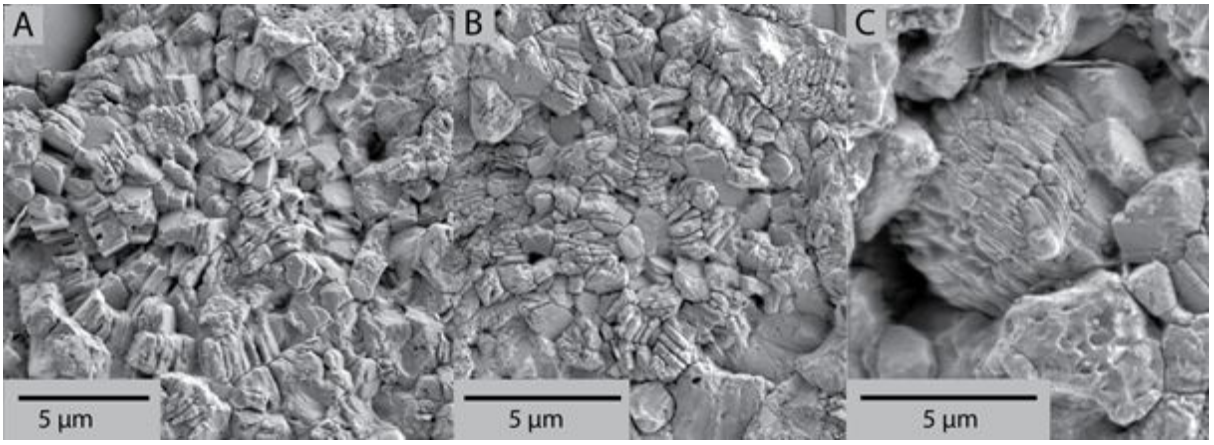


Fig 9 – SEM pictures representing ; A- Biggest *P. triassica* with half of the inner sphere visible composed of thin tabular calcite rhombohedral arranged in parallel group randomly positioned (SO/11). B- *P. triassica* with half of the inner sphere visible composed of block of calcite (STK 1B/29 A). C- Entire *P. triassica* with thin tabular calcite in parallel group visible (ST4/25).

The second Triassic nannoliths, (*Eo*-)*Conusphaera zlambachensis* have low abundance and specimens start to be present at the top of the youngest section, in sample STK 1B/29A (Fig 10, A; 12). Those specimens only seen from one extremity of the cone shape do not vary in shape and size, measuring between 2.25 and 2.94 µm for the length and between 1.57 and 1.96 µm for the width. For the calcareous cysts, *Orthopithonella sp.* (Fig 10, B) and *Thoracosphaera sp.* (Fig 10, C) are rare in the oldest section, but more often present in the youngest samples, and specimens are observed in each section except STK 1A. *Obliquipithonella sp.* (Fig 10, D) are present only in the youngest section STK 1B in low abundance. All those calcareous cysts do not varies in shape, for *Orthopithonella sp.* the size varies between 8.1 and 10 µm, for *Thoracosphaera sp.* between 5.39 µm

and 11.15 µm and for *Obliquipithonella sp.* entire spheres were not visible making the measurement impossible.

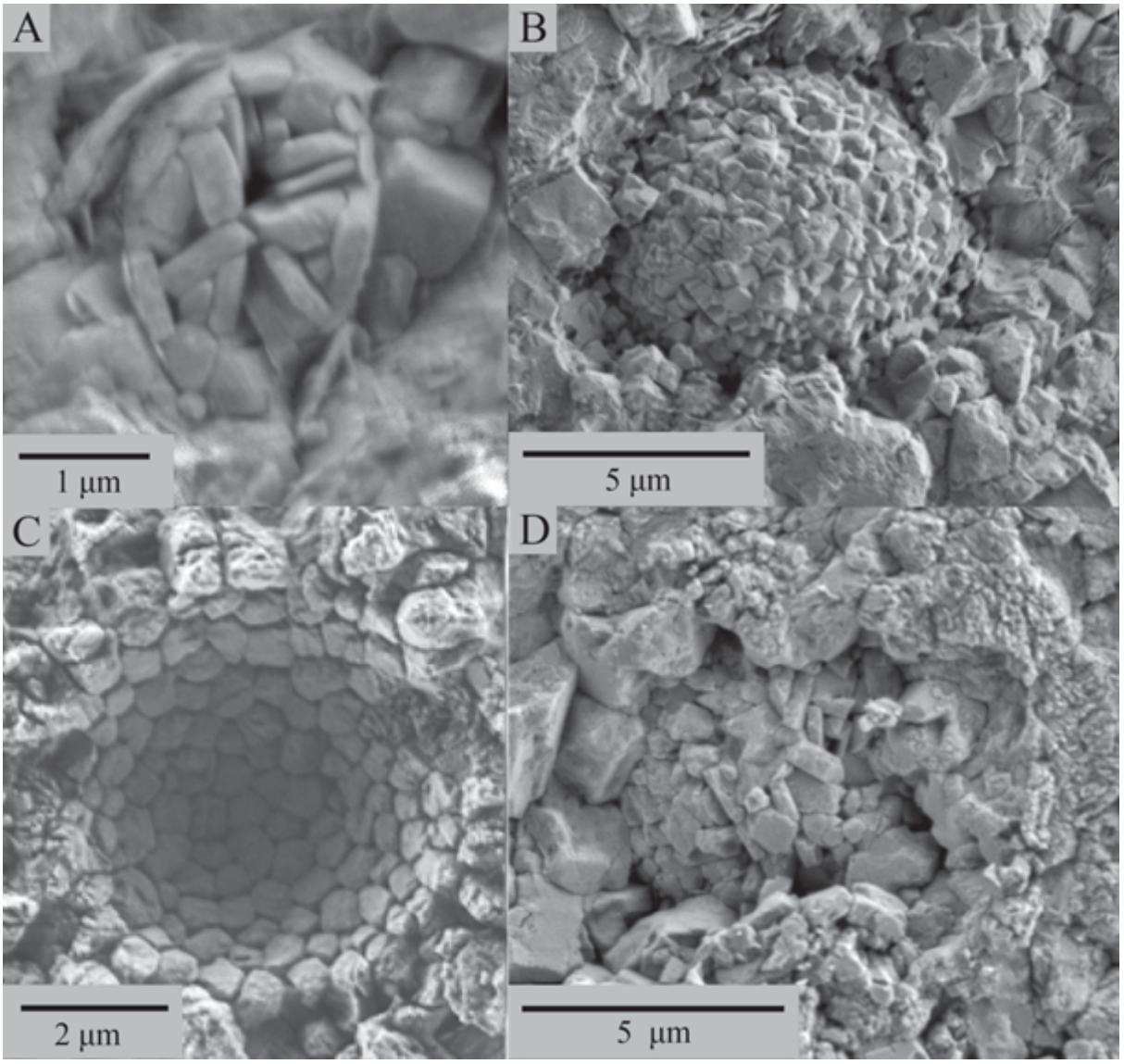


Fig 10 – SEM pictures of A- C. zlambachensis founds in section STK 1B/37B; B- Orthopithonella sp. from ST4/6; C- Thoracosphaera sp. from STK 1A/119A ; D- Obliquipithonella sp. observed in STK 1B/25B.

The assemblage is also composed of some calcispheres observed in low abundance throughout all the sections. They are regular sphere more or less well preserved with a size ranging between 4.32 µm and 9.2 µm (Fig 11, F). Finally, we observed circular structures filled (Fig 11, B, C, D) or not (Fig 11, A, E) of calcite grained randomly arranged and surrounded by various number of axial rays more or less width. Those structures observed often in Sommeraukogel, ST4 sections and rarely in STK sections present a broad range of size going from 8 µm to 17.43 µm. Under the SEM, BackScattered Electrons (BSE) detectors with Energy Dispersive Spectroscopy (EDS) show that the

element’s spectrum is dominated by Ca, O and C, indicating that those structures are composed of calcite.

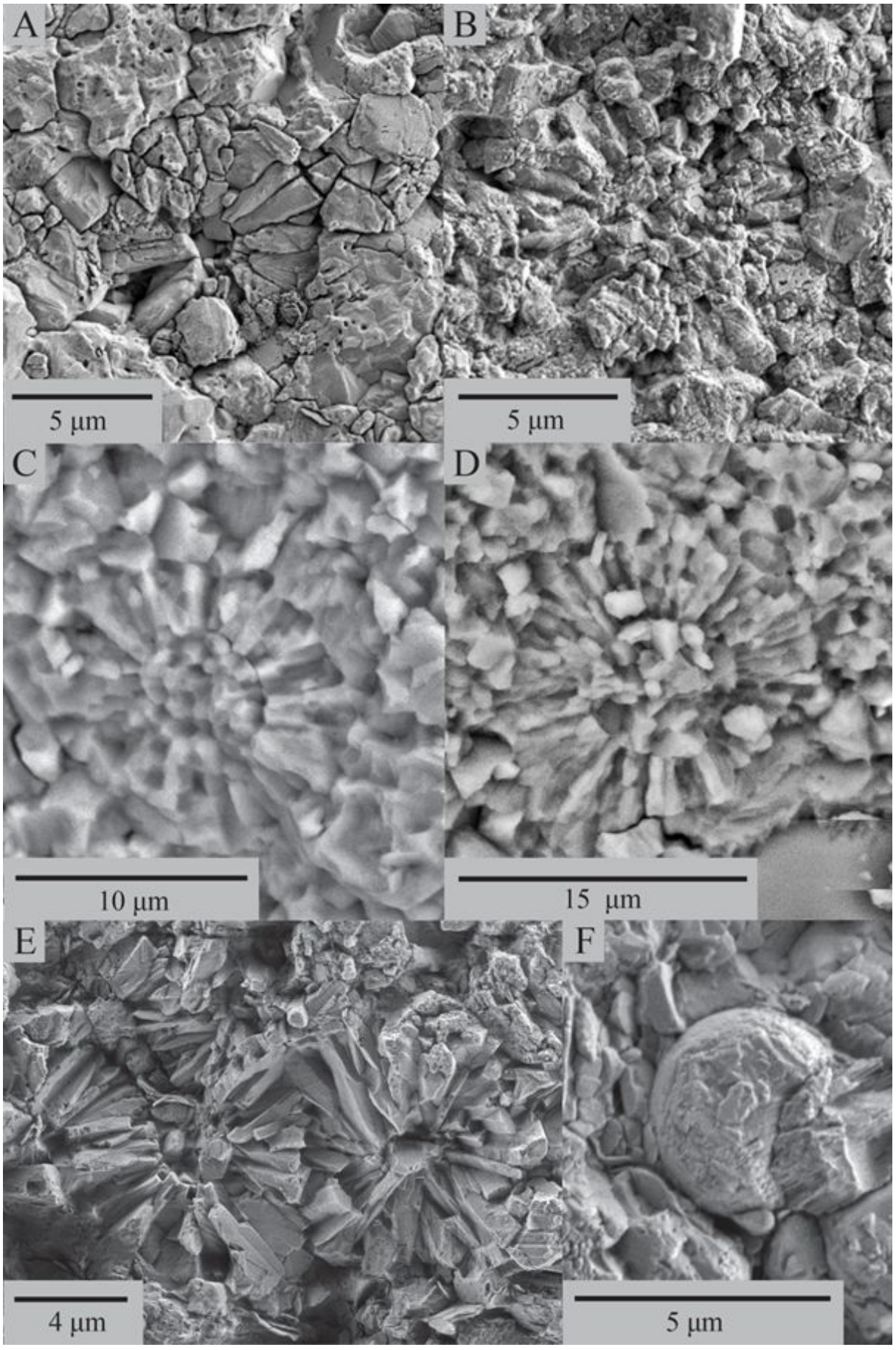
A
5 μm
B
5 μm
C
10 μm
D
15 μm
E
4 μm
F
5 μm

Fig 11 – SEM pictures representing the calcisphere-like with radial rays from samples: A) ST4/25, B) ST4/29, C and D) SO/17, E) ST4/6; F) SEM pictures representing a calcisphere from STK 1B/45.

### c. *P. triassica* abundance and carbonate flux:

The incertae sedis *Prinsiosphaera triassica* is the most abundant calcareous nannofossils in our sections and in general in Upper Triassic sediments (Gardin et al., 2012; Preto et al., 2013a). With a relative abundance above 87% in all samples except for ST4/2 (50%), those species clearly dominate the assemblage. The carbonate flux controlled by the absolute abundance of nannofossils show a global increase during the lowermost Rhaetian and a slight decreased toward the Zlambach Formation (Fig 12). Indeed, until the top of STK 1A section, the values vary between 0,02 and 2 N $10^{-10}$ $cm^{-2}$ $My^{-1}$. This stability is followed by an increased at the base of STK 1B reaching 6 N $10^{-10}$ $cm^{-2}$ $My^{-1}$. Finally, a slight decrease toward the Zlambach Formation with values between 2 and 4 N $10^{-10}$ $cm^{-2}$ $My^{-1}$ characterized the top of the section. The absolute abundance values, from Sommeraukogel until the top of STK 1A varies between 397 and 52719 (*P. triassica*/$cm^2$). They are marked by two major diminutions of abundance, one between samples ST4/6 and 10 with a 42 times decreased and a second between samples ST4/45 and STK 1A/103 with a reduction of factor 31. For the youngest section, STK 1B/C, the abundance varies between 50684 and 148094 (*P. triassica*/$cm^2$). The maximum value occur at the base of the subsection (STK 1B/16). This base of STK 1B presents a major increase with values 14 times more important than the 10944 (*P. triassica*/$cm^2$) at the top of STK 1A. The top of the section shows a gradual decrease of the abundance characterized by a factor 2.7 between the lowest and the top samples. The average diameter of *P. triassica* does not vary significantly through the section (Fig 12).

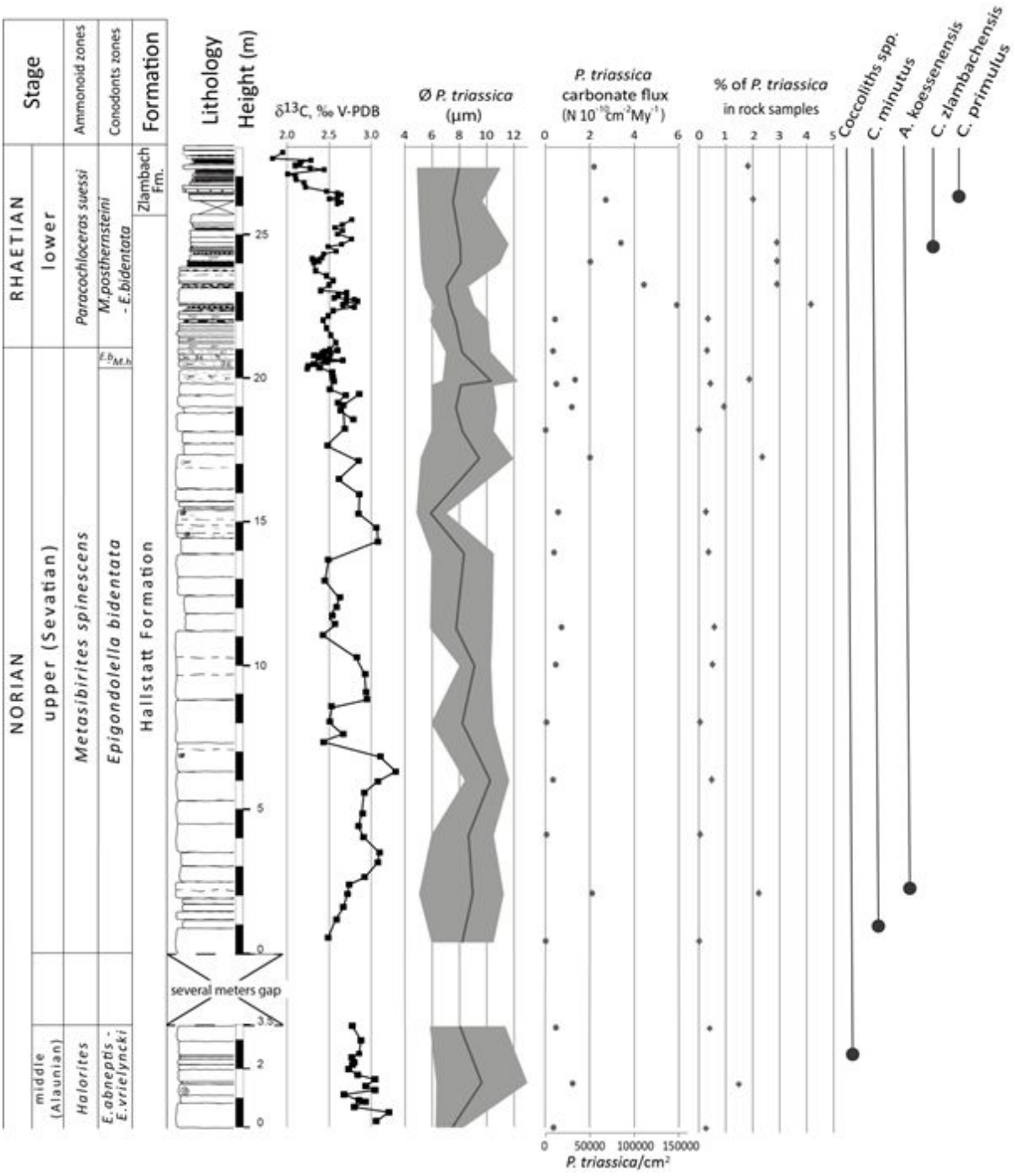


Fig 12 – *P. triassica* $CaCO_3$ paleofluxes (specimens $10^{-10}$ $cm^{-2}$ $My^{-1}$) and absolute number (specimens/$cm^2$) plotted against the lithology, $\delta^{13}C_{carb}$ values, the percentage of *P. triassica* in the rock sample, size measurement of P. triassica with the black line corresponding to the mean diameters and the grey area of the range between minimum and maximum sizes. The lowest occurrences are represented by the black dots and the line above indicate the presence of the species.

**d. Lateral variation:**

Two beds were investigated in order to estimate the lateral variations in the abundance of nannofossils. The two beds (STK 1A/113B and 1C/12E, lower Rhaetian) shows typical assemblages with a dominance of *P. triassica*, rare coccoliths, *Orthopithonella sp.*, *Obliquipithonella sp.* and *Thoracosphaera sp*. The main observations are the strong difference in abundance between the two beds and into every single bed. Indeed, the median values of 105 (total number of nannofossils for 1cm transect under the SEM) of STK 1C/12E is 9 times the median value (12) of STK 1A/ 113B (Fig 13). This last value confirms the low abundance seen during the quantification analysis of the bed STK 1A/113A during the stratigraphic estimation of the variations. Also, for each beds the total number of nannofossils exposed a difference between the minimum and the maximum of 6 times for STK 1A/ 113B and of 3,9 times for STK 1C/12E.

The bed STK 1A/113B shows the highest difference between the minimum and maximum but all values plot below 50. Also, 4 samples on 6 have a total abundance around the median value at 12 (see tab 1). While for the bed STK 1C/12E, the difference between the minimum and maximum is less important but the values are spread between 50 and 200. Moreover, only 3 samples on 8 have close values, samples at 2m, 3m and 8m with respective abundance of 61, 67 and 53 (Tab 1).

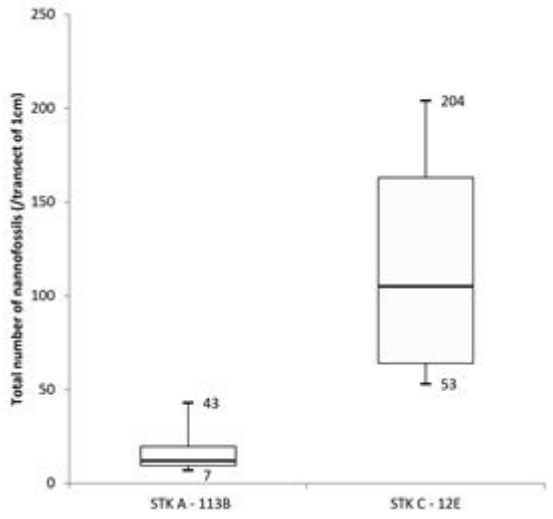


Fig 13 – Box plot representing the total number of nannofossils per transect of 1cm in STK 1A/113 and in STK 1C/12E.

| STK 1A / 113B | | STK 1C / 12E | |
|---|---|---|---|
| | | 1 m | 181 |
| 0 m | 7 | 2 m | 61 |
| 0,6 m | 22 | 3 m | 67 |
| 1 m | 43 | 4 m | 105 |
| 1,5 m | 9 | 5 m | 145 |
| 1,9 m | 13 | 6 m | 204 |
| 2,5 m | 11 | 8 m | 53 |

Tab 1- Quantification values of samples STK 1A/113 and STK 1C/12E.

## *5.* Discussion

### a. Impact of diagenesis:

During the Upper Triassic, Steinbergkogel registered deep-shelf environment, with paleo-depth of at least 300 meters, but probably 500m (Schlager, 1969), thus largely above the lysocline. Some dissolution already occurred in the water column during the sinking of the nannofossils. Also, in such environment the fabric-selective dissolution and overgrowth as observed in our samples might occur during the early stage of diagenesis (Flügel, 2010) immediately after deposition or burial (Berner, 1980). Dissolution features are visible from the base until sample ST4/12. After a transition presenting both patterns, the recrystallization is visible from the sample ST4/38 to the top. As already described by Gardin et al. (2012), some *P. triassica* specimens are affected by dissolution features. If we compare the specimens observed in our section with the classification scale of preservation stages created by Bralower (1991), the best-preserved specimens (stage one) with entire outer layer are absent. The *P. triassica* observed here were all etched from stage two (partly etched outer layer) to stage four (etched inner layer). This nannolith is also impacted by overgrowth features during the early diagenesis, with, crystallization of neocalcite on the whole surface affecting for example a *P. triassica* specimen in section STK 1A (Fig 5, A). This process

occurred also for the calcareous cysts *Orthopithonella* and *Obliquipithonella* which are empty sphere during the life stage and have always been observed filled by calcite crystals. Finally, this recrystallization affected also coccoliths by the overgrowth of the rims and central elements preventing sometime the complete identification of the specimens.

It is assumed that changes in the trace elements composition can occur during the diagenesis (Land and Epstein, 1970; Budd and Land, 1990; Saller and Moore, 1991). Both recrystallization and dissolution can alterate the original signal by adding/removing preferentially trace elements to reach a new equilibrium with the pore water (Brand and Veizer, 1980). As the sediments studied here were deposited in deeper marine environment, none of them could have suffer meteoritic diagenesis. We wanted thus to evaluate rather if early and burial diagenesis could have an effect on the abundance of the nannofossils. To trace potential diagenesis Sr, Na, Mn, Fe can be particularly useful. Differences in partitional coefficients and in composition in marine versus pore water lead to a contrasting evolution of certain elements. Burial diagenesis impact can lead to depleted Sr and Na content and in contrary, to increased Mn and eventually Fe, Zn concentration (Turekian, 1972, Brand and Veizer, 1980). At Steinbergkogel, most of these elements have low concentration. Manganese concentration varies between 22 and 237 ppm, $Na^{+}$/Sr between 220 and 495 ppm with Sr values ranging from 137 to 215 ppm. Iron reaches high concentration; the values are between 385 and 2590 ppm. As noted before Fe and Al shows a strong correlation indicating detrital source for Fe and so this element was excluded when considering diagenesis effects. On the Sr+Na vs. Mn cross-plot no anticorrelation was observed, which would have been expected in case of increased diagenetic impact. Only the 4 samples of STK1B section showed a negligible anticorrelation. Furthermore, the generally low Sr values (average: 162 ppm) are consistent with the depositional environment characterized by low sedimentation rate in deeper settings (Coimbra et al., 2015) and are not the result of loss due to diagenesis. In several middle and upper Jurassic successions with Ammonitico Rosso type sediment similarly low values in the range from 50 to 250 ppm were reported (Price and Sellwood, 1994, Préat et al. 2006, Coimbra et al. (2015). Overall, these values were considered as close to the original signal, supporting a very early diagenesis with a very light influence on the preservation (Price and Sellwood, 1993; Derry, 2010; Coimbra and Olóriz, 2012; Coimbra et al., 2015). This observation is thus also valid for Steinbergkogel with no influence of the diagenesis on the abundance of the nannofossils.

### b. Upper Triassic coccolithophorids:

#### i. Lowest occurences of coccolithophorids

The oldest occurrences of the coccolithophorids have been reported just below the Norian/Rhaetian boundary by Gardin et al. (2012) in sediment from Steinbergkogel. Bown et al.,

(1991) report that the main location of evolutionary activity in both the Late Triassic and Early Jurassic seems to have been the subtropical/tropical Western Tethys region. Also Gardin et al. (2012), suggested the Western Tethys, especially the Austrian Alps as the best place to document the earliest evolution of calcareous nannofossils with probably even older occurrence. In addition, the molecular clocks date the earliest origin of potentially calcifying haptophytes, so called Calcihaptophycidae, at 270-240 Ma for SSU rDNA and at 200 Ma for LSU rDNA (De Vargas et al., 2005). Our results are going in the direction of the dates proposed in those genetic studies. Indeed, we report the oldest occurrence of *coccoliths sp.* in the Alaunian 2 (mid-Norian) in SO/15 (around 220 Ma). This specimen is badly preserved and only third of the rim shape is visible without clear rim elements. With caution, we propose a lowest occurrence of the coccolithophorids sp. at least in the middle Norian. In addition, other rims shapes more doubtful were observed at Sommeraukogel. Above, the specimen observed at ST4/2 (Upper Triassic) have a clear entire protolith rim visible, with a really small size (length of 2.13 µm and width of 1.57 µm) leaving no doubt for its identification as *C. minutus*. Belonging to upper Norian sediments, this specimen of *C. minutus* is the oldest report so far. Until now, the lowest occurrence was reported by Gardin et al. (2012) just above the Rhaetian boundary. Still at the base of this upper Triassic section at ST4/6, a well preserved specimen of *A. koessenensis* was observed with a clear loxolith rim and double bar crossing the central area, corresponding to the oldest *A. koessenensis* report. During our quantification *C. primulus* could not be observed but in the same section Gardin et al. (2012) report the lowest occurrence of this species at STK B/28 corresponding to lower Rhaetian.

### ii. Evolution of early coccolithophorids

The investigation of sediment from mid-Norian until Rhaetian allowed us to follow the early evolution of the coccolithophorids and the nannoliths appearing in the upper Triassic. The evolution trend observed in this study is in agreement with the report of Bown (1987) and Gardin et al. (2012), but in contradiction to Bralower (1991) proposing *C. primulus* as the ancestor. With our proposed order of apparition and the lastest reports (see Bown, 1987; Gardin et al., 2012; Richoz and Krystyn, 2015), we suggest *C. minutus* as the ancestor of *C. primulus*, giving rise to the other genus, *A. koessenensis.* Besides the evolution from protolith-subvertical rim toward a more loxolith rim, this proposed lineage is also logical regarding the size going from a small specimen with *C. minutus* (1,6 to 2,4 µm) to a bigger specimen with *C. primulus* (3 to 5 µm) through the middle size *A. koessenensis* (1,9 to 3,2 µm). The first occurrence of *C. zlambachensis* is slightly after *A. koessenensis* and before *C. primulus*, in agreement with Gardin et al. (2012). During the upper Norian/lowermost Rhaetian the diversification rate of coccolithophorids is very low with only three species described. The diversification seems to be slow with millions years in between each new species apparition

considering a sedimentation rate of 3m/1Ma as proposed by Schlager (1969) for Hallstatt-type sediments. The diversification rate will accelerate only during the early Jurassic, with 1.7 species per million years. It is only during the late Cretaceous, 120 Ma after their apparition that coccolithophorids reach their maximum diversity (Bown et al., 1991).

#### iii. Doubtful *incertae sedis*:

One interrogation remains on the second type of calcisphere possessing axial rays around a central structure (Fig. 11). The mineral composition of those structures indicate $CaCO_3$ composition with pics for Ca, C, O and Mg. The spectrums do not show traces of Si which could be a proof of silica replacement during the diagenetic process. Thus, the hypothesis of siliceous microfossils such as radiolarians, or even diatoms or silicoflagellates could be excluded. The amount of Sr was very low as well, conclusive of a primary calcite structure rather than aragonitic. It was thus probably a undefined calcareous nannofossils species. Such specimen have been reported first by Di Nocera and Scandone (1977), in different Middle to Upper Triassic deep environment sediments from several localities of the Western Tethys (Italy, Austria, Montenegro, and Greece). They were described as *Nannoconus sp.* with a circular shape and an axial canal. This one was irregularly filled with calcite and surrounded by radial structure probably formed by recrystallization. Later, Bellanca et al. (1993) reports similar structures in Sicilian sections of Carnian age and arguing for a strong link to *Nannoconus sp*. Those *Nannoconus sp.* have conical or spherical shape composed of plates spirally arranged around a canal, which is close to the *incertae sedis* shape presented here. However, it is important to highlight that the *Nannoconus sp.* are known only from the Upper Jurassic, which is more than 50 Ma later (Bown and Cooper, 1998). Recently, in Upper Carnian sediment from Italy, Preto et al. (2012; 2013a; 2013b) described those kind of specimens first as *Thoracosphaera sp*. then as calcispheres interpreted as calcareous dinocysts, from the "*Pithonella*" group, with epitaxial overgrowth as a consequence of the diagenesis. They explain these forms as a recrystallization artefact with crystals rays growing in open space, with rhombohedral terminations. However, we did not observed any of these rhombohedral terminations. It is thus not possible from our data to decipher if these specimens were recrystallised calcareous dynocysts (Preto et al., 2012; 2013a; 2013b) or very early appearance of *Nannoconus sp*. (Nocera and Scandone, 1977; Bellanca et al. 1993).

### c. Upper Triassic Nannofossils quantification:

During quantification of nannofossils, one of the potential caveat is the effect of dissolution/overgrowth on the absolute abundance. The impact of the dissolution on the nannofossils can be strong but is very specific dependent for dissolution occurring above the lysocline (e.g., Berger, 1973; Roth and Berger, 1975; Thierstein, 1980; Gibbs et al., 2004). In Steinbergkogel, Gardin

et al. (2012) hypothesized that variation of the preservation could impact the primary biological signal. Our careful control on diagenesis (see above) demonstrate however that if dissolution and overgrowth do have an influence on the preservation of the specimens, there are not affecting their abundance. This is confirmed by the fact that three samples with different abundance present similar dissolution features.

### i. Lateral variation

The lateral variation into two beds, show clear change in abundance inside the same bed. The lateral variation is not often investigated during nannofossils quantification. In the Triassic time, Maurer et al. (2003) studied compositional variations of calciturbidites regarding the lithology and fossils assemblages and abundance in a basinal succession of the Dolomites (Southern Alps). They found a lateral variation of the fossils assemblages' link to a difference in lithology and they explain those results by a sorting effect in turbidity currents. The two beds investigated in Steinbergkogel correspond to a Hallstatt facies presenting no turbiditic events. Also, the influence of seafloor current (i.e. contourite) is nowadays often called to explain variation in assemblages and in abundances in deep-sea sedimentation (Rebesco et al., 2014). However, as report by different authors (e.g., Johnson and Johnson, 1969; Ivanova et al., 2016), the bottom currents are sorting the microfossils and the grains by size showing a link between the two. In Steinbergkogel, investigation of thin-sections (Richoz et al., 2012, Richoz and Krystyn, 2015), did not suggest any sorting of the grains, thus potential bottom current does not seem to be the right explanation. The most consistent hypothesis is the temporal variation. Indeed, even if the sample belongs to the same beds, they could have been collected at a few millimeters or centimeters of differences higher or lower along the same transect. As report by Schlager (1969), the sedimentation rate at Steinbergkogel is very slow with 3 meters deposed in 1Ma. Thus, 3 mm of difference in the sampling position, would create a variation of 1000 years between the ages of the two samples. This could explain such variation in the abundance results of those two beds and by consequence the second-order increases and decreases in the quantification of *P. triassica*.

### ii. *P. triassica* abundance and carbonate flux:

The nannofossils assemblage observed in Steinbergkogel is typical for Upper Triassic sediments with all the Upper Triassic species described present. Moreover, as observed in all the previous study of nannofossils during the Upper Triassic in the Western Tethys (Fisher et al., 1976; Wiedmann et al., 1979; Jafar, 1983; Gardin et al., 2012; Preto et al., 2013a), the nannoliths *P. triassica* is fully dominating the assemblage with a relative abundance above 85% in most of samples. The paleoflux from the main nannoliths of the Upper Triassic is important to estimate the contribution

of those pelagic calcifiers to the carbonate production. The progressive increase of *P. triassica* along the Upper Norian to reach 6 (N $10^{-10}$ $cm^{-2}$ $My^{-1}$) across the N/R boundary highlight the transition from *P. triassica*-poor to *P. triassica*-rich period predicting the success of those nannoliths in the Late Rhaetian. Indeed, even if the abundance of *P. triassica* only reach 4.2% per volume of rock in the early Rhaetian, the carbonate contribution of *P. triassica* increase by a factor of 15 just after the N/R boundary, corresponding to a first step before to reach the rock-forming abundance described by Preto et al. (2013a) in the late Rhaetian. The factors boosting this croissance are still not yet understood. This first increase is quickly followed by the slight decrease in abundance occurring at the end of the section. This diminution co-occurs with the first occurrence of the second Upper Triassic nannoliths *C. zlambachensis* and a change in lithology with the transition to the Zlambach Formation. Those two observations raise the question of a possible competition between those two nannoliths and/or a possible negative feedback of the eutrophication occurring with the marly input of the Zlambach Formation. Indeed, nannoplanktons are sensitive to changes in the trophic levelThe change to a more marly lithology, possibly parallel to an increase in the nutrient concentration could have been unfavourable for *P. triassica*.

Our quantification results are in accordance with the semi-quantitative values of Gardin et al. (2012) during the same time interval and at the same place. However, our percentages of *P. triassica* per volume of rock during the Norian in deep-shelf paleo-settings are slightly lower than the results published by Preto et al. (2013a) in shallow sea (Pizzo Mondelo) and open marine settings (Pignola-Abriola). For those two studies the time equivalence is only possible between ST4 and *M. bidentata*, *M. hernsteini*, *P. andrusovi* Zones (Norian). For ST4, our percentages are really low between 0.01 and 2.3 % (Fig 12). Preto et al. (2013a) report at Pizzo Mondelo (Sicanian Basin, Sicily – shallow sea) stable values below 3% during *M. bidentata* Zone (base of ST4), follow by an increase to 20% during *M. hernsteini*, *P. andrusovi* Zones (top of ST4). At Pignola-Abriola (Lagonegro Basin – Open Marine), Preto et al. (2013a) present values trending in opposition than the previous locality. Indeed at the end of *M. bidentata* Zone the volume percentages of *P. triassica* is around 10% and decrease below 5% during *M. hersteini*, *P. andrusovi* Zones (top of ST4). Note, that the analysis methods were different. Preto et al. (2013a) by using point-counting method obtained results for a surface resulting in a overestimation of the calculated amount per $cm^3$, while we calculated a percentage for a volume of rock, with an equation underestimating the real abundance per $cm^3$. Moreover, in our study only the complete specimens were counted, while Preto et al. (2013a) counted even the small single elements interpreted as broken *P. triassica*. During the late Rhaetian, at Pizzo Mondelo (Sicanian Basin, Sicily) they characterized *P. triassica* as rock-forming nannofossils with an abundance reaching up to 60% of the rock volume. At Pignola-Abriola, the maximum abundance occurring only in the *M. ultima* Zone is lower, around 20%. In consequence, Preto et al. (2013a)

suggested that *Prinsiosphaera* was more common in shallower environment (Pizzo Mondello, Sicanian Basin) than in open marine setting (Pignola-Abriola, Lagonegro Basin). If *P. triassica* is effectively present during the whole time studied, it become a relevant composant only in the lowermost Rhaetian (around 4-5%), with some changes just after the N/R boundary interval. However, the success time of *P. triassica* will be later in the upper Rhaetian. . The analysis of a sample from Eiberg section (NCA), corresponding to an intraplatform basin of the Upper Rhaetian confirm the observation of Preto et al., (2013). The quantification of this sample follows the preparation and calculation method developed in this study, shows that in the Upper Rhaetian in Eiberg *P. triassica* represent 30% of the rock in $cm^3$ and 45 % of the rock-surface in $cm^2$. The increase to rock-forming describe by Preto et al. (2013a), occurred only from the late Rhaetian but is preceded by at least one 15 fold increase during the lower Rhaetian as described above.

### iii. *P. triassica* size evolution:

Concerning the size of *P. triassica*, first data published by Bralower (1991) point out a size increase from 6 µm during the Mid-Norian to 9 µm in the upper Rhaetian. Then, Clémence (2010) described a size reduction during the latest Rhaetian with size ranging from < 5 µm up to 10 µm. In our samples, the size range is broad and vary from 4.93 µm to 12.92 µm (Fig 9). This last maximum size is 3 µm and 4 µm bigger than the biggest specimens seen respectively by Clémence (2010) and Bralower (1991). In our dataset such size is not an exception because several specimens bigger than 11 µm have been measured. The size increased seen by Bralower (1991) and the size decreased during the Late Rhaetian seen by Clémence (2010) have not been observed in this study during the Norian to Early Rhaetian, but our data come from a time-frame between these two studies.. The size is in general stable along all the sections with only few minor quick variations between one sample to another.

## Conclusions

This detail quantitative investigation of the 3 sub-sections at Steinbergkogel, a candidate GSSP for the Norian–Rhaetian boundary, with an approach including careful diagenesis evaluation point out the relevance of this locality and in general of the Western Tethys to document the early evolution of the coccolithophorids. The results of this study highlight:

1. ICP-OES analysis shows only early marine diagenesis with a weak impact on the quantification results.
2. The lowest occurrence of *coccoliths sp.* leads in the middle Norian (SO/15).

3. The oldest *C. minutus* and *A. koessenensis* were observed in the Upper Norian (Base of ST4).
4. *C. primulus* was first observed from the Lower Rhaetian (Top of STK 1B).
5. The evolution of the first coccolithophorids is slow, from the ancestor *C. minutus* then *C. primulus, giving the rise to A.koessenensis in between*. The size increase throughout this evolution and the rim structure evolve from protolith-subvertical rim to loxolith rim.
6. The incertae sedis, *Prinsiosphaera triassica* is dominating the calcareous nannofossils abundance during Upper Triassic.
7. The increase in abundance of *P. triassica* from the Upper Norian to the lower Rhaetian is interpreted as the beginning of their success in the late Rhaetian, but this nannoliths is still not rock-forming at this time.

**Acknowledgements** This research was granted by the Austrian Science Foundation (Project P 29497-P29 to Sylvain Richoz). Dorothee Hippler is acknowledge for her help for ICP-OES measurements and their analyses. Franz Tscherne for his work during the preparation of the SEM samples.

**References**

Armstrong, H., Brasier, M.D., 2005: Microfossils. Malden. Oxford. Carlton. Blackwell Publishing, Second Edition, 296.

Bellanca, A., Di Stefano, E., Di Stefano, P., Erba, E., Neri, R., Pirini Radrizzani, C., (1993): Ritrovamento di ‘‘Calcisfere’’ e nannofossili calcarei in terreni carnici della Sicilia. Paleopelagos, 3, 91 – 96.

Berger, W.H., (1973): Deep-sea carbonates: Evidence for a coccolith lysocline. Deep Sea Research, 20, 917 – 921.

Berner, R.A., (1980): Early diagenesis as a theoretical approach. – Princeton, Princeton University Press, Princeton Series in Geochemistry, 241.

Bittner, A. (1890): Die Brachiopoden der alpinen Trias. – Abhandlungen der kaiserlich – königlichen geologischen Reichsanstalt, 14, 252.

Bordiga, M., (2015): Absolute nannofossil abundance estimates: Quantifying the pros and cons of different techniques – Revue de micropaléontologie, 58, 155 – 165.

Bornemann, A., Aschwer, U., Mutterlose, J., (2003): The impact of calcareous nannofossils on the pelagic carbonate accumulation across the Jurassic – Cretaceous boundary. Palaeogeography, Palaeoclimatology, Palaeoecology, 199, 187 – 228.

Bown, P.R., (1985): Archaeozygodiscus gen. nov. and other Triassic coccoliths. INA Newsletter 7, 32 – 35.

Bown, P.R., (1987): The structural Development of Early Mesozoic Coccoliths and its Evolutionary and Taxonomic Significance. Abh. Geol. B.-A, 39, 33 – 49.

Bown, P.R., Burnett, J.A., Gallagher, L.T., (1991): Historical Biology: An international Journal of Paleobiology. 5:2-4, 279 – 290, doi: 10.1080/10292389109380407.

Bown, P.R., (1998). Triassic. In: Bown, P.R. (Ed), *Calcareous nannofossil biostratigraphy*. London, Chapman & Hall, British micropalaeontological Society Publication Series, 315, 29 – 33.

Bown, P.R., Cooper, M.K.E., (1998). Jurassic. In: Bown, P.R. (Ed), Calcareous nannofossil biostratigraphy. London, Chapman & Hall, British Micropalaeontological Society Publication Series, 315, 34 – 85.

Bralower, T.J., Bown, P.R., Siesser, W.G., (1991): Significance of Upper Triassic nannofossils from the Southern Hemisphere (ODP Leg 122, Wombat Plateau, N.W. Australia) – Marine Micropaleontology, 17, 119 – 154.

Brand, U., Veizer, J., (1980): Chemical diagenesis of a multicomponent carbonate-system – 1: trace elements. J. Sed. Petrol., 50, 1219–1236.

Budd, D.A., Land, L.S., (1990): Geochemical imprint of meteoric diagenesis in Holocene ooid sands, Schooner Cays, Bahamas: correlation of calcite cement geochemistry with extant groundwaters. J. Sed. Petrol., 60, 361 – 378.

Chayes, F., (1954): The theory of thin-section analysis. Journal of Geology, 62, 92 – 101.

Clémence, M.E., Gardin, S., Bartolini, A., Paris, G., Beaumont, V., Guex, J., (2010): Bentho-planktonic evidence from the Austrian Alps for a decline in sea-surface carbonate production at the end of the Triassic. Swiss Journal of Geosciences, 103, 293 – 315.

Coimbra, R., Olóriz, F., (2012): Geochemical evidence for sediment provenance in mudstones and fossil-poor wackestones (Upper Jurassic, Majorca Island). Terra Nova, 24, 437 – 445.

Coimbra, R., Immenhauser, A., Olóriz, F., Rodríguez-Galiano, V., Chica-Olmo, M., (2015): New insights into geochemical behavior in ancient marine carbonates (Upper Jurassic Ammonitico Rosso): Nivel poxies for interpreting sea-level dynamics and palaeoceanography. Sedimentology, 62, 266 – 302.

Derry, L.A., (2010): A burial diagenesis origin for the Ediacaran Shuram-Wonoka carbon isotope anomaly. Earth and Planetary Science Letters, 194, 152 – 162.

De Vargas, C., Aubry, M.P., Probert, I., Young, J., (2005): Origin and evolution of coccolithophores: from coastal hunters to oceanic farmers. In: Falkowski, P.G., Knoll, A.H. (Eds), Evolution of Aquatic Photoautotrophs, Boston, Elsevier, 251 – 285.

Di Nocera S., Scandone P., (1977): Triassic nannoplankton limestones of deep basin origin in the central Mediterranean region. Palaeogeography Palaeoclimatology Palaeoecology, 21, 101 – 111.

Fisher, A.G., Honjo, S., Garrison, R.A.E., (1976): Electron Micrographs of Limestones and their Nannofossils. Princeton, Princeton University Press, 157.

Flügel, E., (2010): Microfacies of carbonate rocks. Analysis, Interpretation and Application. Berlin, Springer-Verlag, 976.

Gardin, S., Krystyn, L., Richoz, S., Bartolini, A., Galbrun, B., (2012): Where and when the earliest coccolithophores? – Lethaia, 45, 507 – 523.

Gibbs, S.J., Shackleton, N.J., Young, J.R., (2004): Identification of dissolution patterns in nannofossil assemblages: A high-resolution comparison of synchrnous records from Ceara Rise, ODP Leg 154. Paleoceanography, 19, PA1029.

Goddéris, Y., Donnadieu, Y., De Vargas, C., Pierrehumbert, R.T., Dromart, G., Van de Schootbrugge, B., (2008): Causal or casual link between the rise of nannoplankton calcification and tectonically-driven massive decrease in Late Triassic atmospheric $CO_2$? – Earth and Planetary Science Letters, 267, 247 – 255.

Hornung, T., Krystyn, L., Brandner, R., (2007): A Tethys-wide mid-Carnian (Upper Triassic) carbonate productivity decline: Evidence for the Alpine Reingraben Event from Spiti (Indian Himalaya)? – Journal of Asian Earth Sciences, 30/2, 285 – 302.

Hüsing, S.K., Deenen, M.H.L., Koopmans, J.G., Krijgsman, W., (2011): Magnetostratigraphic dating of the proposed Rhaetian GSSP at Steinbergkogel (Upper Triassic, Austria): Implications for the Late Triassic time scale. – Earth and Planetary Science Letters, 302, 203 – 216.

Ivanova, E., Murdmaa, I., Borisov, D., Dmitrenko, O., Levchenko, O., Emelyanov, E., (2016): Late Pliocene-Pleistocene stratigraphy and history of formation of the loffe calcareous contourite drift, Western South Atlantic. Marine Geology, 372, 17 – 30.

Jafar, S.A., (1983): Significance of Late Triassic calcareous Nannoplankton from Austria and Southern Germany. Neues Jahrbuch für Geologie und Paläeontologie, 166, 218 – 259.

Janofske, D., (1987): Kalkige Nannofossillien aus der ober-Trias (Rhät)der Nördlichen kalkalpen. Berliner geowiss. Abh, 86, 45 – 67.

Johnson, D.A., Johnson, T.C., (1969): Sediment redistribution by bottom currents in the central Pacific. Deep-Sea Research, 17, 157 – 169.

Jordan, R.W., 2009. Coccolithophores. In: Schaechter, M. (Ed). Encyclopedia of Microbiology. Third Edition. Oxford, Elsevier 5, 593 – 605.

Kenter, J.A.M., Schlager, W., (2009): Slope angle and basin depth of the Triassic Platform-Basin Transition at the Gosaukamm, Austria. Austrian Journal of Earth Sciences, 102, 15 – 22.

Kittl, E. (1912): Materialien zu einer Monographie der Halobiidae und Monotidae der Trias. Palaeontologie der Umgebung des Balatonsees, 2(4), 10 pl, 1 – 129.

Krystyn, L., (1980): Triassic conodont localities of the Salzkammergut region (Northern Calcareous Alps) – Geologischen Bundesanstalt, 35, 60 – 98.

Koken, E. (1897): Die Gastropoden der Trias um Hallstatt. – Abhandlungen der kaiserlich – königlichen geologischen Reichsanstalt, 17, 1 – 112.

Krystyn, L., Richoz, S., Gallet, Y., Bouquerel, H., Kürschner, W.M., Spötl, C., (2007a): Updated bio-and magnetostratigraphy from Steinbergkogel (Austria), candidate GSSP for the base of the Rhaetian stage. – Albertiana, 36, 164 – 173.

Krystyn, L., Bouquerel, H., Kuerschner, W.M., Richoz, S., Gallet, Y., (2007b): Proposal for a candidate GSSP for the base of the Rhaetian stage. – New Mexico Museum of Natural History and Science, Bulletin, 41, 189 – 199.

Land, L.S., Epstein, S., (1970): Late Pleistocene diagenesis and dolomitization, North Jamaica. Sedimentology, 14, 187 – 200.

Leitner, C., Neubauer, F., Urai, J.L., Schoenherr, J., (2011): Structure and evolution of a rocksalt-mudrock-tectonite: the haselgebirge in the Northern Calcareous Alps. Journal of Structural Geology, 33, 970 – 984.

Mandl, G.W., (2000): The Alpine sector of the Tethyan shelf - Examples of Triassic to Jurassic sedimentation and deformation from the Northern Calcareous Alps. – Mitteilungen der Österreichischen Geologischen Gesellschaft, 92, 61 – 78.

Maurer, F., Reijmer, J.J.G., (2003): Quantification of input compositional variations of calciturbidites in Middle Triassic basinal succession (Seceda, Dolomites, Southern Alps). International journal of Earth Sciences, 92, 593 – 609.

Mojsisovics, E.V., (1873, 1875, 1902): Das Gebirge um Hallstatt. Die Mollusken-Faunen der Zlambach- und Hallstätter Schichten; Suppl.: Die Cephalopoden der Hallstätter Kalke. – Abhandlungen der Geologischen Reichsanstalt, 6: H1(1873), H2(1875), Suppl.(1902).

Monteiro, F.M., Bach, L.T., Brownlee, C., Bown, P., Rickaby, R.E.M., Poulton, A.J., Tyrell, T., Beaufort, L., Dutkiewicz, S., Gibbs, S., Gutowska, M.A., Lee, R., Riebesell, U., Young, J., Ridgwell, A., (2016): Why marine phytoplankton calcify – Science Advance, 2, e1501822.

Mosher, L.C., (1968): Triassic conodonts from western North America and Europe and their correlation. – Journal of Paleontology, 42/4, 895 – 946.

Ogg, J.G., (2012): Triassic. In: Gradstein, F.m., Ogg, J.G., Schmitz, M.D., Ogg, G.M. (Eds), The Geologic Time Scale 2012, Amsterdam. Elsevier, 1176, 681 – 730.

Préat, A., Morano, S., Loreau, J. P., Durlet, C., Mamet, B., (2006): Petrography and biosedimentology of the Rosso Ammonitico Veronese (middle-upper Jurassic, north-eastern Italy). Facies, *52*(2), 265 – 278.

Preto, N., Kustatscher, E., Wignall, P.B., (2010): Triassic climates – State of the art and perspectives – Palaeogeography, Palaeoclimatology, Palaeoecology, 290, 1 – 10.

Preto, N., Rigo, M., Agnini, C., Bertinelli, A., Guaiumi, C., Borello, S., Westphal, H., (2012): Triassic and Jurassic calcareous nannofossils oft he Pizzo Mondello section: A SEM study. Rivista Italiana di Paleontologia e Stratigrafia, 118, 131 – 141.

Preto, N., Agnini, C., Rigo, M., Sprovieri, M., Westphal, H., (2013a): The calcareous nannofossil Prinsiosphaera achieved rock-forming abundances in the latest Triassic of western Tethys: consequences for the $\delta^{13}C$ of bulk carbonate – Biogeosciences, 10, 6053 – 6068.

Preto, N., Willems, H., Guaiumi, C., Westphal, H., (2013b): Onset of significant pelagic carbonate accumulation after the Carnian Pluvial Event (CPE) in the western Tethys – Facies, 59, 891 – 914.

Price, G.D., Sellwood, B.W., (1993): Palaeotemperatures indicated by Upper Jurassic (Kimmeridgian – Tithonian) fossils from Mallorca determined by oxygen isotope composition. Palaeogeography, Palaeoclimatology, Palaeoecology, 110, 1 – 10.

Prins, B., (1969): Evolution and stratigraphy of coccolothinids from the lower and middle lias. International Conference Planktonic Microfossils, Geneva, 2, 547 – 558.

Prins, B., (1971): Speculations on relations, evolution and stratigraphic distribution of discoasters. In: Farinacci, A. (Editor), *Proceedings of the Second Planktonic Conference Roma 1971*. 2 Edizioni Tecnoscienza, Rome, 1017 – 1037.

Rebesco, M., Hernández-Molina, F.J., Van Rooij, D., Wåhlin, A., (2014): Contourites and associated sediments controlled by deep-water circulation processes: State-of-the-art and future considerations. Marine Geology, 352, 111 – 154.

Richoz, R., Krystyn, L., Von Hillebrandt, A., Martindale, R., (2012): End-Triassic crisis events recorded in platform and basin of the Austrian Alps. The Triassic/Jurassic and Norian/Rhaetian GSSPs – Journal of Alpine Geology, 55, 321 – 374.

Richoz, S., Krystyn, L., (2015): The Upper Triassic events recorded in platform and basin of the Austrian Alps. The Triassic/Jurassic GSSP and Norian/Rhaetian GSSP candidate – Berichte der Geologischen Bundesanstalt, 111.

Robinson, P.L., (1973): Paleoclimatology and continental drift. In: Tarling, D.H., Runcorn, S.K. (Eds.), Implications of continental drift to the Earth Sciences. New York, Academic Press, 1184, 449 – 476.

Rood, A.P., Hay, W.W., Barnard, T., (1973): Electron microscope studies of lower qnd middle Jurassic coccoliths. Eclogae geol. Helv., 66/2, 365 – 382.

Roth, P.H., and Berger, W.H., (1975): Distribution and dissolution of coccoliths in the South and central Pacific. Foraminiferal Research, Spec. Publ., 13, 87 – 113.

Ruffell, A., Simms, M.J., Wignall, P.B., (2015): The Carnian Humid Episode of the late Triassic: a review. Geological Magazine, 153, 271 – 284.

Saller, A.H., Moore, C.H., (1991): Geochemistry of meteoric calcite cements in some Pleistocene limestones. Sedimentology, 38, 601 – 621.

Schlager, W., (1969): Das Zusammenwirken von Sedimentation und Bruchtektonik in den triadischen Hallstätterkalken der Ostalpen. – Geologische Rundschau, 59, 289 – 308.

Schorn, A., Neubauer, F., (2014): The structure of the Hallstatt evaporite body (Northern Calcareous Alps, Austria): A compressive diapir superposed by strike-slip shear? – Journal of Structural Geology, 60, 70 – 84.

Suchéras-Marx, B., Giraud, F., Mattioli, E., Gally, Y., Barbarin, N., Beaufort, L., (2014): Middle Jurassic coccolith fluxes: A novel approach by automated quantification. Marine Micropaleontology, 111, 15 – 25.

Thierstein, H., R., (1976): Mesozoic calcareous nannoplankton biostratigraphy of marine sediments. Marine Micropaleontology, 1, 325 – 362.

Thierstein, H., R., (1980): Selective dissolution of Late Cretaceous and earliest Tertiary calcareous nannofossils: Experimental evidence. Cretaceous Research, 2, 165 – 176.

Turekian, K.K., (1972): Chemistry of the Earth. Holt, Rinehart, Winston, New-York, 131.

Tyrrell, T., Young, J.R., (2009): Coccolithophores. In: Steele, J.H., Turekian, K.K, Thorpe, S.A. (Eds). Encyclopedia of Ocean Sciences. Oxford, Elsevier, 3900, 606 – 614.

Wiedmann, J., Fabricius, F., Krystyn, L., Reitner, J., Ulrichs, M., (1979): Über Umfang und Stellung des Rhaetian. Newsletter on Stratigraphy, 8, 133 – 152.

Young, J.R., Ziveri, P., (2000): Calculation of coccolith volume and its use in calibration of carbonate flux estimates, Deep Sea Research, II, 47, 1679 – 1700.

Zeebe, R. E. & Westbroek, P. (2003): A simple model for the CaCO3 saturation state of the ocean: the "Strangelove", the "Neritan", and the "Cretan" Ocean. Geochemistry, Geophysics, Geosystems 4, 1 – 26.